CHAPTER – I

CHAPTER – I

1 INTRODUCTION

1.1 X-rays

X-rays were invented in 1895 by a German physicist named Wilhelm Conrad Röntgen. He noticed that a fluorescent screen in his laboratory began to glow when the tube was turned on. This surprised him because he thought that the heavy cardboard surrounding the tube would catch most of the radiation. This shows that X-rays penetrate most materials. X-rays have been used as powerful tools in analytical, physical, chemical, biological and structural characterization of matter. For example, X-ray fluorescence is widely used in qualitative element analysis. X-ray photoelectron spectroscopy (XPS) can be used to study the electronic structure of materials and X-ray crystallography provides three-dimensional structures of crystalline material at atomic resolution. Various X-ray scattering technique can yield structural information for amorphous materials at varying degrees of resolution. Since the production and the properties of X-rays are intimately related to electrons. X-rays have also contributed substantially to the development of solid state physics and nuclear physics. In fact, almost all areas of physics, from atomic physics to astrophysics, have received significant contributions through the application of X-rays. Today, almost a century after the momentous discovery, X-rays continue to be of fundamental importance not only in physics but also in other areas of science and technology.

X-rays are electromagnetic waves, like light waves having wavelength range from ~25Å to 0.025 Å, i.e., energy range from ~500 eV to 500 KeV. A commonly used source of X-rays is the X-ray tube (Coolidge type), which consists of a thermionic cathode and an anode made of copper or tungsten (i.e., high Z metal) enclosed in a highly evacuated glass tube. Electrons emitted from cathode are accelerated and then made to strike the anode. X-rays are emitted from the anode surface as a consequence of its bombardment by the energetic electron stream. The energy spectrum of X-rays, so produced, consists of continuous spectrum of radiation on which peaks of sharply defined energies, i.e., characteristic X-rays, are superimposed.

1.2 Production of X- rays

X-rays are produced by two main mechanisms and come in two varieties - characteristic and bremsstrahlung x-rays.

1.2.1 Characteristic X-rays

Electrons are the same whether orbiting in shells around the nucleus, or produced inside an X-ray generator. Whenever their velocity or position is changed, there is a loss of energy that takes a radiative form (X-rays). When electrons travelling at the target have their direction changed, a spectrum of X-rays results. However the electrons circulating in the atoms can also change.

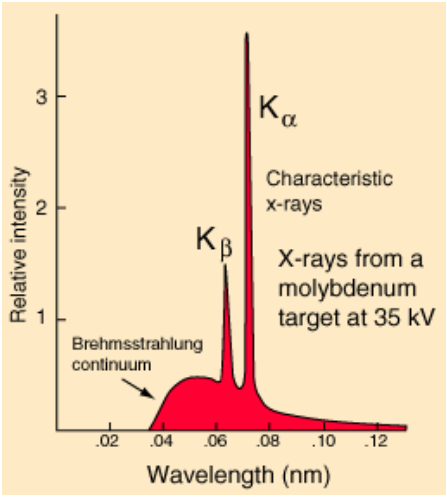

Figure 1-1 Characteristics X-rays

While most of the electrons have their path changed and little else, some will collide with electrons. Sufficient energy in such collisions can result in the ejection of an orbiting electron. 'Sufficient energy' means enough to overcome the bonding energy of the orbiting electron. The impacting electron will move off with reduced energy, and the ejected electron will move off in a different direction and speed with the remaining energy, there is an empty position in one of the shells. The remaining orbiting electrons will 'pack down' to fill the hole, and when changing orbits will lose energy and emit this as radiation. The orbiting levels are fixed as a physical property fixing the elemental identity of an atom, and so the energy emission will be **characteristic** of that atom. The energy will be mono-energetic and so appear as a

spike rather than a continuous spectrum. Electrons ejected come from the K, L or M orbits. The other corollary of this type of interaction is that the atom becomes an ion (it has lost an ejected electron!).

All atoms will produce characteristic radiation but not all are visible in the xray portion of the electromagnetic spectrum. Elements with higher atomic numbers have their K, L, M or N shells of sufficient energy to be called 'X-rays'. The discrete characteristic radiation energies are equal to the difference in the energy level of the outer and inner orbital electrons.

The X-ray energy is proportional to the atom's Z. Where the incident electrons have energies less than the electron binding energy, there will be no characteristic radiation emitted. As the electron energy increases past the threshold level, the maximum level of characteristic radiation reaches 20% of total production, and then starts to fall to 10% in the 50-100 KeV range and 3% in the 200 KeV range. In the megavoltage range, characteristic radiation is negligible.

1.2.2 Bremsstrahlung X-rays

Bremsstrahlung is a German word meaning “braking radiation” which describes the process of x-ray generation. The high speed electron impacts on the target and at the atomic level approaches the nucleus. There is no actual collision between electron and nucleus because the electron interacts with the Columbic nuclear forces and its vector quantities of direction and velocity are changed. Since kinetic energy derives from velocity ($KE=\frac{mv^2}{2}$). The change in energy is radiated as electromagnetic radiation. The amount of energy means a short wavelength within the x-ray band.

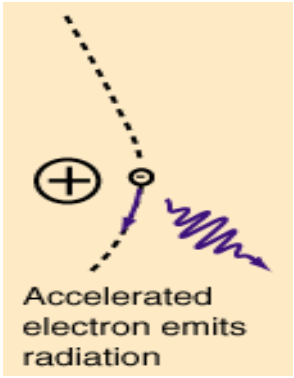

Figure 1-2 Bremsstrahlung X-rays

As the electron is not destroyed, it can undergo multiple interactions, and even initial interactions will vary from minor to major energy changes depending on the actual angle and proximity of attack, and the point of 'impact' on the nucleus. As a result, bremsstrahlung radiation will have continuous spectrum where the maximum energy relates to the entire KE of the electron but will be infrequent. The energy spectrum without filtration is a straight line that matches the formula

$$I_{E=} kZ(Em-E)$$

where I_E = intensity of photons of energy E, *k* is a constant, Z is the atomic number of the target, Em is the maximum photon energy which is numerically equal to the applied kilovolts peak (kVp).

The average energy of a bremsstrahlung-derived beam is approximately 1/3 of the maximum energy.

The direction of bremsstrahlung X-rays is decidedly horizontal. Where the energy of the incident electron beam is around 100 KeV, bremsstrahlung production has a spatial orientation described as 'anisotropic' that is equally in all directions.

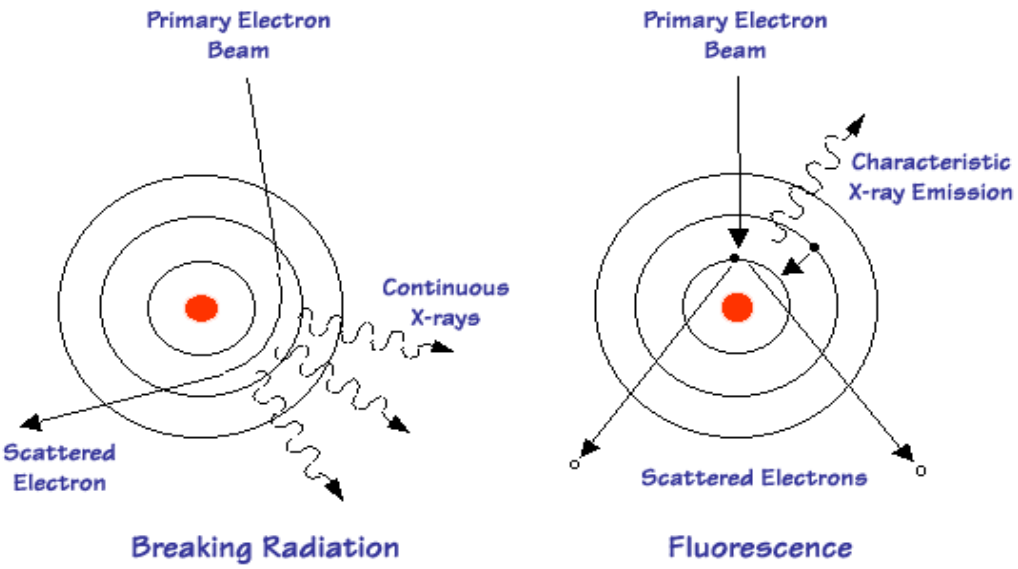

Figure 1-3 X-ray production

1.3 X-rays from Synchrotron

Synchrotron radiation was seen for the first time at General Electric in the United States in 1947 in a different type of particle accelerator (synchrotron). It was first

considered a nuisance because it caused the particles to lose energy, but it was then recognized in the 1960s as light with exceptional properties that overcame the shortcomings of X-ray tubes.

In the mid- to late 1970s, scientists began to discuss ideas for using synchrotrons to produce extremely bright X-rays. These discussions led to the construction in the late 1980s and early 1990s of the ESRF and shortly thereafter two other "third-generation" synchrotrons (the Advanced Photon Source in the United States and SPring-8 in Japan). Impressive progress continues to be made in accelerator physics, electronics and computing as well as in magnet and vacuum technologies, with the goal of producing even brighter and more stable X-rays.

Synchrotron radiation is the name given to the radiation which is emitted when charged particles are accelerated in a curved path or orbit. In the circular particle accelerators like synchrotrons, where charged particles are accelerated to very high speeds, the radiation is referred to as synchrotron radiation. This radiated energy is proportional to the fourth power of the particle speed and is inversely proportional to the square of the radius of the path. If the electrons in circular motion have energies more than 1 GeV then the radiations emitted are X-rays. However, the synchrotron radiation consists of only continuous X-rays and no characteristic X-rays. Charged particles do not radiate while in uniform motion, but during acceleration a rearrangement of its electric fields is required and this field perturbation, travelling away from the charge at the velocity of light, is what we observe as electromagnetic radiation. Free accelerated electrons radiate similarly.

In synchrotron radiation sources (storage rings) highly relativistic electrons are stored to travel along a circular path for many hours. Radiation is caused by transverse acceleration due to magnetic forces in bending magnets (forming the circular path) or periodic acceleration in special insertion device magnets like undulators, wiggler magnets and wavelength shifters. The radiation is emitted in pulses of 10 - 20 psec separated by some 2 nsec or longer separation if desired.

Due to the relativistic energy of the particles the generated light has the following characteristics -

(i) The emitted **continuous spectrum** is of **high intensity**.

(ii) The natural **divergence** of the radiation is very small and collimators further reduce these values.

(iii) Distinct linear or circular **polarization**, which can be selected depending on the application, is of particular interest in investigations of magnetic systems.

(iv) Synchrotron radiation has a **time-structure**, because the particles are stored in pulses. This time-structure can be used to investigate time dependent phenomena like relaxation or diffusion. The time scale ranges from nanoseconds to many hours.

Monochromator selects very fine energy bands and thus provides selectivity to elements and even to the chemical state of an element. The radiation spectrum is continuous and the energy can be freely chosen according to the system under investigation (**tunability**). X-rays penetrate easily into and even through matter and therefore **non-destructive investigations** have become of special interest.

Due to the high intensity, recording of a spectrum is very fast. Measurements can therefore be carried out during processing the material under investigation. These **in-situ experiments** provide information about the processes which take place during the transformation of the sample.

1.4 Absorption of X-rays

When a beam of X-rays falls onto an absorber, a number of different processes may occur (Fig.1.4). When the X-rays hit a sample, the oscillating electric field of the electromagnetic radiation interacts with the electrons bound in an atom. Either the radiation will be scattered by these electrons or absorbed and excite the electrons.

A narrow parallel monochromatic X-ray beam of intensity $\mathbf{I_0}$ passing through a sample of thickness **x** will get a reduced intensity **I** according to the expression:

$$\ln (I_0 / I) = \mu x \qquad (1.1)$$

where μ is the linear absorption coefficient, which depends on the types of atoms and the density ρ of the material. At certain energies where the absorption increases drastically and gives rise to an absorption edge. Each such edge occurs when the energy of the incident photons is just sufficient to cause excitation of a core electron of the absorbing atom to a continuum state, i.e. to produce a photoelectron. Thus, the energies of the absorbed radiation at these edges correspond to the binding energies of electrons in the K, L, M, etc, shells of the absorbing elements. The absorption edges are labeled in the order of increasing energy, K, L_I, L_{II}, L_{III}, M_I,…., respectively.

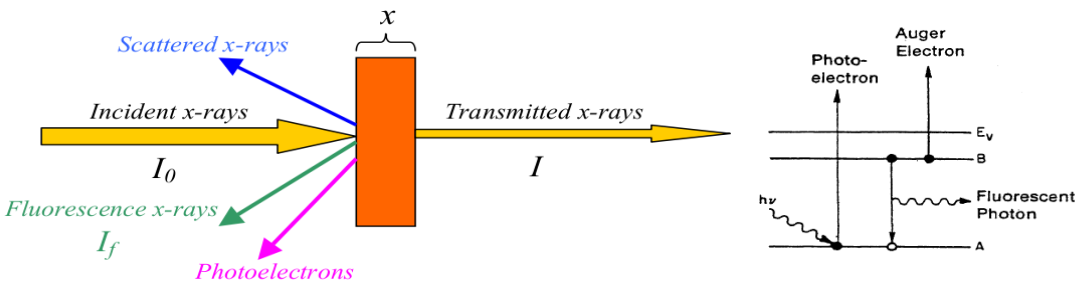

Figure 1-4 Absorption processes for X-rays

The difference between I and I_0 for a fixed wavelength is dependent on the thickness of the absorber and on the linear absorption coefficient μ, which is a constant related to the absorbing materials. Since all the absorption process shown in figure 1.4 ultimately depends on the presence of electrons, clearly the ability of a material to absorb electromagnetic radiation is related to the density of electrons. The linear absorption coefficient of a material, therefore, depends on the types of atoms present and the density of the material. Thus, μ/ρ is characteristic of each element at any specified wavelength.

The absorption coefficient will decrease smoothly with higher energy, except for special photon energies. When the photon energy reaches the critical value for core electron transition, the absorption coefficient increases abruptly.

1.5 X-ray absorption fine structure

X-ray absorption fine structure (XAFS) is a powerful and versatile technique for studying structures of materials in chemistry, physics, biology, and other fields. It is a widely-used technique for determining the local geometric and/or electronic structure of matter. XAFS spectra are sensitive to the formal oxidation state, coordination chemistry, and the distances, coordination number and species of the atoms immediately surrounding the selected element. XAFS provides a practical, and relatively simple, way to determine the chemical state and local atomic structure for a selected atomic species. XAFS can be used in a variety of systems and bulk physical environment. XAFS is routinely used in a wide range of scientific fields, including biology, environmental science, catalysts research, and material science[1].

[1] Frenkel A I, Murthy V and Newville M, 2001, J Synchrotron Rad., **8**, 669

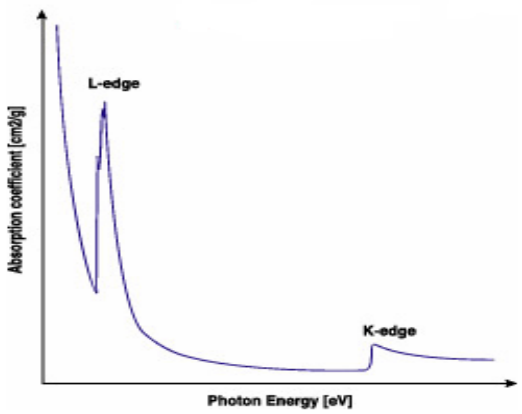

Figure 1-5 X-ray absorption coefficient vs photon energy

If the absorption coefficient is plotted as a function of E (Fig. 1.5), the experimental data show three general features: (1) an overall decrease in X-ray absorption with increasing energy; (2) the presence of a sharp rise at certain energies called edges, which roughly resembles step-function increases in the absorption and (3) above the edges, a series of wiggles or oscillatory structure that modulate the absorption, typically by a few percent of the overall absorption cross section.

The first feature is illustrative of the well-understood quantum-mechanical phenomenon of X-ray absorption by atoms, as described, for example, by Fermi's ''golden rule'' in standard texts[2]. The energy position of the second feature is unique to a given absorption atom and reflects the excitation energy of inner-shell electrons. Each absorption edge is related to a specific atom present in the material and, more specifically, to a quantum-mechanical transition that excites a particular atomic core-orbital electron to the free or unoccupied continuum levels (ionization of the core orbital). The relationship between the X-ray absorption edges and the corresponding excitation of core electrons is shown in fig. 1.6. Shown are the excitations corresponding to the K, L, and M X-ray absorption edges. The arrows show the threshold energy difference of each edge. Any transitions higher in energy (to unoccupied states above the Fermi energy E_F) are also allowed. The nomenclature for X-ray absorption reflects this origin in the core orbital. For example, K edges refer to transitions that excite the innermost 1*s* electron. The transition is always to unoccupied states, i.e., to states with a photoelectron above the Fermi energy, which leaves behind a core hole. The resulting excited electron is often referred to as a photoelectron and in a solid generally has enough kinetic energy to move freely

[2] Messiah A., 1966, *Quantum Mechanics* (Wiley, New York).

through the material. This occurs even in insulators, since the excited states are almost always extended states (quasifree states in molecules and conduction band states in solids). The energies of the edges (or ionization energies) are unique to the type of atom that absorbs the X-ray, and hence themselves are signatures of the atomic species present in a material.

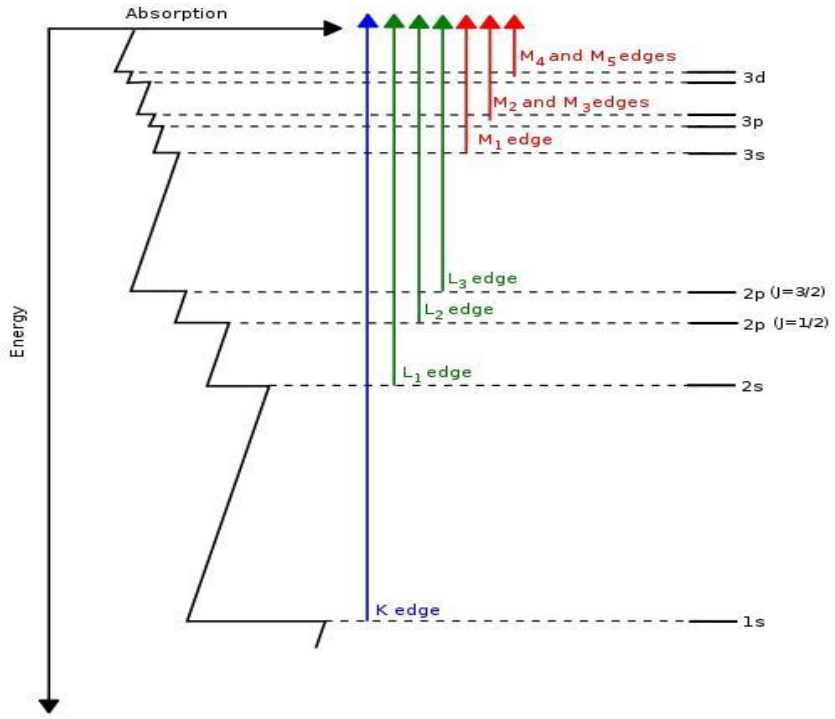

Figure 1-6 The relationship between the X-ray absorption edges and the corresponding excitation of core electrons.

The third feature is the XAFS that is of primary interest in this research. When interpreted correctly, this feature contains detailed structural information, such as interatomic distances and coordination numbers. The generally weak oscillatory wiggles (Fig. 1.7) beyond about 30 eV above the absorption edge were eventually termed EXAFS[3] (Extended X-ray Absorption Fine Structure). This fine structure contains precise information about the local atomic structure around the atom that absorbed the X-ray.

[3] Lytle F. W., Sayers D. E. and Stern E. A., 1975(a), Phys. Rev. B, **11,** 4825.

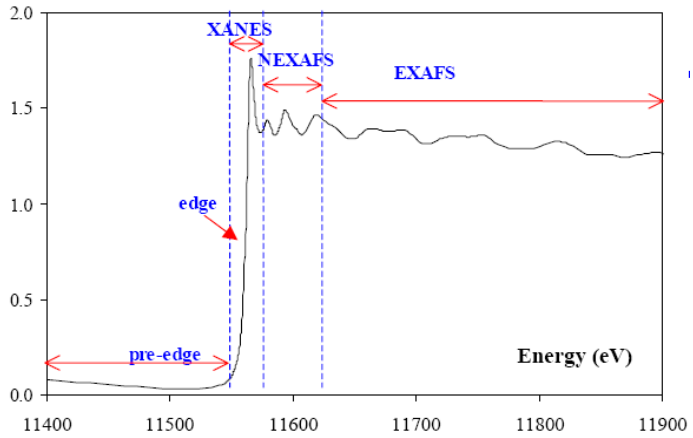

Figure 1-7 The normalized K-absorption spectrum of copper metal showing the pre-absorption, XANES and EXAFS regions

In contrast, the region closer to an edge is often dominated by strong scattering processes as well as local atomic resonances in the X-ray absorption and is generally not as readily interpreted as EXAFS. This region of strong scattering is referred to as the X-ray absorption near-edge structure or XANES and typically lies within the first 30 eV of the edge position. The more general term XAFS was introduced by Rehr et al[4] to refer to the fine structure in both XANES and EXAFS, following the recognition that they both have a common origin, namely, the scattering of a photoelectron by its environment.

The XAFS spectrum χ is defined phenomenologically as the normalized, oscillatory part of the X-ray absorption above a given absorption edge (fig. 1.8), i.e.

$$\chi(E) = [\mu(E) - \mu_0(E)] / \Delta\mu_0 \qquad (1.2)$$

Where $\mu_0(E)$ is the smoothly varying atomic-like background absorption (including contributions, if any, from other edges), and $\Delta\mu_0$ is a normalization factor that arises from the net increase in the total atomic background absorption at the edge in question. In practice, this normalization factor is often approximated by the magnitude of the jump in absorption at the edge. The error in this approximation can be accounted for by a small (typically about 10%) correction to the XAFS Debye-Waller factor, which is called the McMaster correction[5].

[4] Rehr J.J., Alber R.C., Natoli C.R. and Stern E.A., 1986, Phys. Rev. B, **34(6)**, 4350
[5] De Leon J M, Stern E A and Sayers D E, (eds.), 1988, *Proceeding of the V international conference on X-Ray Absorption Fine Structure XAFS V* (Seattle, WA, USA), Physica B, **158**.

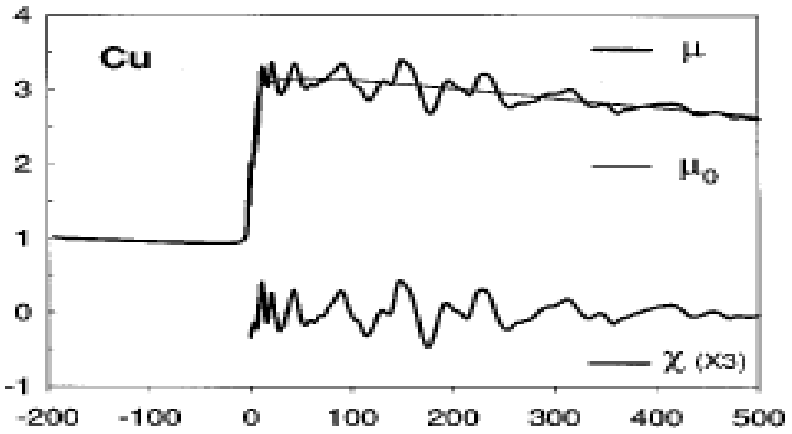

Figure 1-8 The relationship between the X-ray absorption coefficient $\mu(E)$, the smooth atomic like background $\mu_0(E)$, and $\chi(E)$ for a Cu K edge.

The sudden rise in absorption at the edge occurs when an incident X-ray photon has just sufficient energy to cause transition of an electron from the 1s state of some element in the sample to an unfilled state of predominantly p-character (i.e. angular momentum $l = 1$ with respect to the central absorbing atom) (Fig. 1.9). In the present research we shall concentrate on K-edge absorption for simplicity.

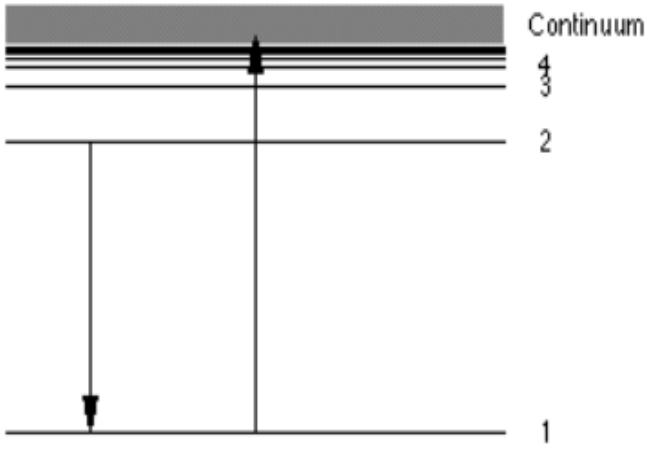

Figure 1-9 Excitation of photoelectron from 1S state to continuum.

Although the XAFS phenomenon and its basic explanation in terms of a quantum mechanical interference effects have been known since the 1930's, the phenomenon did not become a practical experimental tool until two events occurred: the distillation by Sayers, Stern, and Lytle[6] of the essential physics of the process into the standard XAFS equation and their proposal of a simple method of data analysis;

[6] Sayers D.E., Stern E.A., and Lytle F.W., 1971, Phys. Rev. Lett., **27**, 1204.

and the availability of tunable, high flux, high energy-resolution synchrotron radiation beamlines. The number of XAFS experiments performed has grown exponentially since 1970 as a consequence of these developments. The amount of information available from a single XAFS spectrum (typically 10-20 or so parameters) is small compared to that available from X-ray diffraction, but the information available from a well-chosen experiment can be particularly incisive and may be inaccessible by any other technique. XAFS (a short-range order technique) is particularly powerful when intimately combined with complementary techniques such as X-ray diffraction (a long range order technique). Recent developments in theory and experiment show great promise for extending the range and power of the XAFS.

The simplest XAFS experiments are done in transmission mode (fig. 1.10). Polychromatic X-rays are produced by a synchrotron radiation source or by bremsstrahlung from a conventional laboratory source, and a desired energy band of approximately 1 eV bandwidth is then selected by diffraction from a silicon double crystal monochromator. Only those X-ray photons that are of the correct wavelength λ ($\lambda = hc/E$, where h is Planck's constant and c is the speed of light) to satisfy the Bragg condition $n\lambda = 2d\sin\theta$ at the selected angle θ will be reflected from the first crystal and the others are absorbed. The parallel second crystal is used as a mirror to restore the beam to its original direction. The monochromatic X-rays are then allowed to pass through the sample, which should absorb approximately 50% - 90% of the incident X-rays. The incident and transmitted X-ray fluxes are monitored, usually with gas ionization chambers.

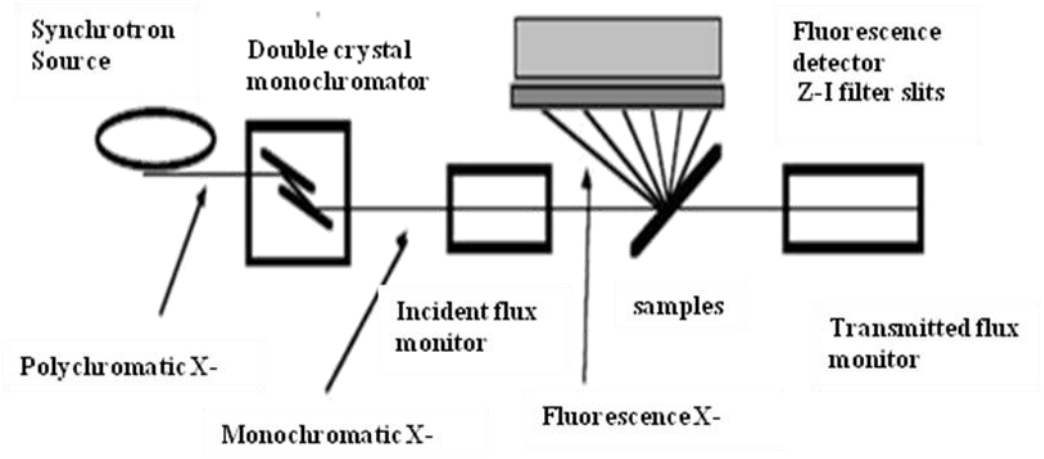

Figure 1-10 Schematic of XAFS experiment

1.5.1 Different features of X-ray absorption spectra

A typical XAS (X-ray absorption spectrum) can be divided into four regions. (Fig.1.7)

(a) Main edge **(b) Pre edge**

(c) XANES **(d) EXAFS**

(a) Main edge region:

In this region, there is a sharp increase in the absorption, when the incident photon energy is equal to or greater than the binding energy (E_0) of the core electron. This increase in the absorption is usually attributed to the transition to empty states in the continuum. The absorption edge is taken as the first inflection point. The shift in E_0 in different compounds gives information about change in valance state of the central atom. The edge is traditionally named depending on the shell from which the electron is ejected i.e. K, L, M edges correspond to the excitation of an electron from K, L, M states respectively. Compared to K-edges, the L-edges occur at lower X-ray energies because they corresponding to the transitions from less bound levels. Fig. 1.7 shows the X-ray absorption spectrum of Cu with four regions.

(b) Pre-Edge region:

Before the absorption edge, certain absorption features appear about 10 eV below the edge. These features are sensitive to the local symmetry, bond length and orbital occupancy. These features, in the case of copper K-edge occur mainly because of quadruple transitions, overlapping of the d-orbital of the absorbing atom with that of the p-orbital of the neighboring oxygen atoms, mixing of the 3d states of the parent absorbing atom with 4p states of neighboring atoms and also band structure effects.

(c) X-ray Absorption Near Edge Structure (XANES) and Near Edge X-ray Absorption Fine Structure (NEXAFS) region:

In the edge region, where photon energy, $E \leq E^0$+10 eV (E^0 is the ionisation energy) the XANES (X-ray Near Edge Structure) is observable. NEXAFS (Near-Edge X-ray Absorption Fine Structure) region is between E^0+10>E $\leq E^0$+50 eV. It has to be noted, that sometimes there is no division between the XANES and NEXAFS region, and the two acronyms are used as synonyms, although NEXAFS is usually used in connection with organic molecules and surfaces. Today, the term NEXAFS is

typically used for soft X-ray absorption spectra and XANES for hard X-ray spectra. (Fig. 1.11(a)).

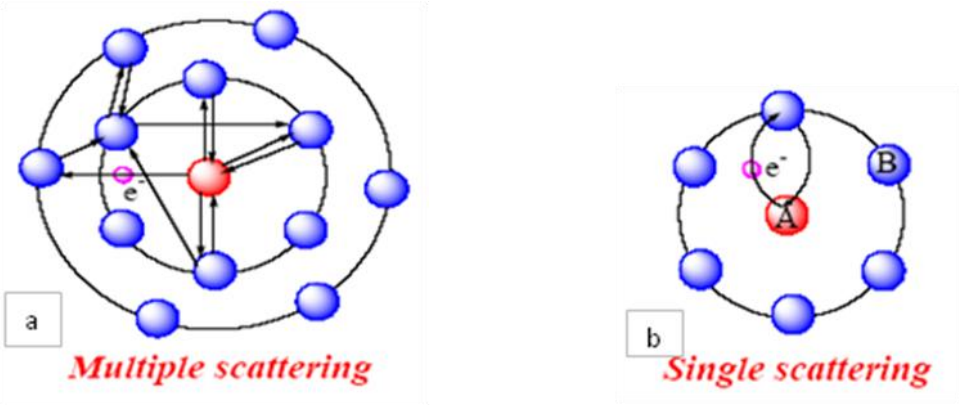

Figure 1-11 (a) multiple scattering processes responsible for XANES; (b) Single scattering processes responsible for EXAFS.

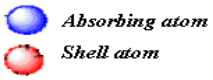

(d) EXAFS (Extended X-ray absorption Fine structure Studies) region:

The region starts from about 50 eV above the edge and extends typically up to several hundred electron volts. Here, the photoelectrons have high kinetic energy ($E-E_0$ is large), and single scattering by the nearest neighboring atoms normally dominate. The fine structure observed in this region is mainly because of interference of the outing wave and the backscattered wave (from the neighboring atoms) representing the state of the ejected photoelectrons. EXAFS phenomenon is thus a final state effect of the ejected photoelectron from the absorbing atom[7]. (Handbook of Synchrotron Radiation, 1983). The phenomenon of EXAFS has been known for more than sixty years. The early explanations for EXAFS met with limited success and hence the power of EXAFS for structure determination was not realised. Only recently has EXAFS been established as powerful tool for structure determination and also for extraction of other physical information not easily obtained from other techniques such as X-ray and neutron diffraction. The EXAFS oscillations result from the interference of the outgoing photoelectron back-reflected from neighbouring atoms. (Fig. 1.11(b)) The interference depends upon the phase difference between the

[7] Stern E. A. and Heald S. M., 1983, *Handbook on Synchrotron Radiation*, Vol. 1, edited by Koch E E, Elsevier Science Ltd, North-Holland, p. 955.

two interfering wave functions and hence the oscillations in μ depends upon the distances of nearest-neighbour atoms from the absorption atom. The amplitude of the backscattered wave depends upon the number and type of backscattering atoms, and thus EXAFS oscillations also depends upon the number and type of nearest neighbours. EXAFS can therefore be used to get valuable information like the number of nearest-neighbour atoms, the type of nearest-neighbour atoms, the relative displacements of theses atoms about their mean positions and the nearest-neighbour bond lengths. Information about next nearest-neighbours and so on can also be obtained if the experimental data is of sufficiently good quality. Since absorption edges of different elements are well separated in energy, one can selectively probe the local environment around each atomic species. The sensitivity of EXAFS to local structural means that EXAFS can be applied to almost all types of materials crystalline and amorphous solids, disordered materials, liquids, supported catalysts, gases etc. EXAFS has now become an indispensable tool in several areas of physics, chemistry, materials science and biochemistry.

Extended X-ray absorption fine structure EXAFS is an experimental technique that provides local order information around a given atom with high surface sensitivity[8]. This is due to the extremely small extinction length of the evanescent wave appearing when the probe beam shines the sample in total reflection conditions[9]. The noticeable advantage of this technique is that we may use the X-ray absorption spectroscopy a bulk probe to investigate surface effects. In particular, the technique permits the analysis of buried interfaces systems that are difficult to be analyzed even with more sophisticated surface investigation equipment. Applications of EXAFS can be found in literature on a variety of fields, namely, chemical reactions at the solid state[10] surface treatments[11] and structural studies of thin films[12]. A variety of spectrometers dedicated to this method is available on the major synchrotron radiation sources[13].The theory of X-ray absorption spectroscopy is presently well understood and it permits the quantitative determination of local structure parameters both from the near edge region as well as from the extended zone.

[8] Teo B. K., 1986, *EXAFS*: *Basic Principles and Data Analysis*, Inorganic Chemistry Concepts, Vol. 9 (Springer-Verlag, Berlin). Fornasini P., *Introduction to X-ray absorption spectroscopy*, 2003, in: S. Mobilio and G. Vlaic (Eds.) *Synchrotron Radiation: Fundamentals, Methodologies and Applications*, Conference Proceedings, Vol. 82, SIF, Bologna, pp. 129–170.
[9] Parratt, L. G., 1959, Rev. Mod. Phys., **31**, 616.
[10] Acapito D., Davoli I., Ghigna P., and Mobilio S., 2003, J. Synchrotron Radiat., **10**, 260.
[11] Hecht D., Borthen P., and Strehblow H. H., 1996, Surf. Sci., **365**, 263.
[12] Jiang D. T., Alberding N., Seary A. J. and Crozier E. D., 1988, Rev. Sci. Instrum., **59**, 60.
[13] Oyanagi H., Owen I., Grimshaw M., Head P., Martin M. and Saito M., 1995, Rev. Sci. Instrum., **66**, 5477.

1.5.2 Applications of XAFS

XAS is an experimental technique used in different scientific fields including molecular and condensed matter physics, materials science and engineering, chemistry, earth science, and biology. In particular, its unique sensitivity to the local structure, as compared to X-ray diffraction, has been exploited for studying amorphous solids and liquid systems, solid solutions, doping and ion implantation materials for electronics, local distortions of crystal lattices, organometallic compounds, metalloproteins, metal clusters and catalyser.

1.6 The absorption edge

The absorption edge energy is defined as a specific energy of the absorption edge spectrum. The edge energy for an element in a higher oxidation state is usually shifted by up to several electron volts to a higher X-ray energy. In a neutral atom, the positive charge of the nucleus is screened by the negative charge of the electrons. In an atom of higher oxidation state with fewer electrons than protons, the energy states of the remaining electrons are lowered slightly, which causes the absorption edge energy to increase. That is, an X-ray with slightly greater energy is required to excite the core electron. The change in element oxidation state is usually accompanied by a change in Centro symmetry, which will change the features of the absorption edge. The X-ray photon absorbed ($h\nu$) results in transitions within the atomic energy levels of the absorbing atom. During the spectroscopic scan, no absorption occurs until the photon has an energy equal to the ionization energy of core electrons.(Fig. 1.12) At lower X-ray energies, X-ray induced ionization of 2p or 2s electrons gives rise to what are called L_{III}, L_{II}, and L_I absorption edges. At significantly higher X-ray energies, photo ionization of a 1s electron gives rise to the K-absorption edge. For a given element, K edge energies depend slightly (± a few eV) on the chemical environment of the element. For example, higher oxidation state metals have higher positive charge, making it slightly more difficult to photo dissociate a 1s electron, shifting the K edge to higher energy. Shifts of 1-2 eV per oxidation state are typical for first-row transition metals.

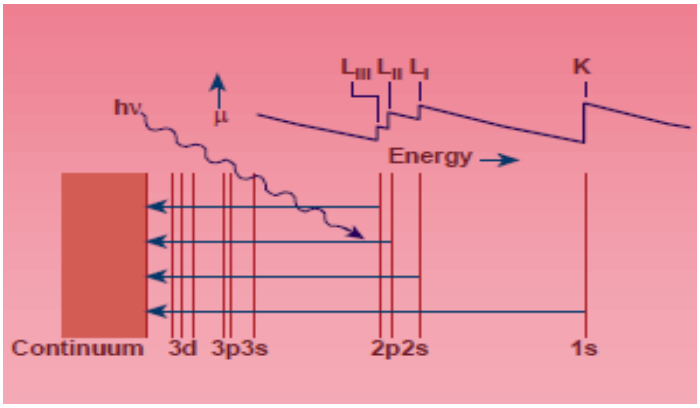

Figure 1-12 XAS Edge result from core ionization

Also, spectroscopic transitions from the 1s orbital to orbital just below the continuum (Fermi level), such as 3d, 4s, 4p, etc., obey electric dipole selection rules like any other electronic transition and assignments of such features can provide information about molecular symmetry. X-ray photons can be scattered either elastically or inelastically. The well-known phenomenon of X-ray diffraction occurs due to interference effects resulting from elastic scattering of X-ray photons by an array of atoms in a material. In inelastic or Compton scattering, the photon loses energy upon scattering from loosely bound electrons. However, scattering effects are negligible when characteristic X-ray absorption takes place, i.e., when an X-ray photon is absorbed and bound electron is excited to an available high-energy state. When the energy of an X-ray photon is close to the binding energy E_0 of a core electron in an atom, the absorption suddenly increases as the core electron is removed from its shell, giving rise to a sharp increase in the absorption coefficient. This is known as the absorption edge. One speaks of a K-edge, when an electron from a K-shell is removed, L-edges when electrons from L-shells are removed, and so on. Different process occurs near this energy, giving rise to several features. The absorption edge structure often consists of discrete absorption bands superimposed on the steeply rising continuum absorption edge. These discrete absorption bands are caused by transitions of core electrons to discrete bound valence levels. The absorption edges that are of most interest are the K-edge (1s – 3p), followed by the three L-edges: L_1-edge (2s – 5p), L_2-edge ($2p_{1/2}$ – $5d_{3/2}$) and L_3-edge ($2p_{3/2}$ – $5d_{5/2}$). These edges are element specific and shifts to higher energies when the atomic number increases. Since the core levels depend on the element and its chemical environment, they also show chemical specificity. X-ray absorption spectroscopy is therefore not only an element specific technique, but it is also sensitive to the

immediate environment of the absorbing atom. X-ray energy range of 3 – 30 keV results in accessibility of K-edges from roughly chlorine to silver. The L-edge of elements from molybdenum through the actinides also falls within this energy range. Radiation in the range of 0.1 – 3 keV will make it possible to do XAS studies of the lower atomic number elements such as carbon, nitrogen and oxygen. The availability of third generation synchrotron sources now allows the routine performance of XAS investigations using K absorption edges occurring even above 30 KeV. Measurements made at absorption edges in the energy range 40 KeV to 90 KeV have successfully been accomplished. That means that XAS spectrum at K-edge of lead (88.0 KeV) has been measured.

1.7 Theory of XANES

The X-ray absorption near edge structure (XANES) is an element-specific electron spectroscopic technique which is highly sensitive to bond angles, bond lengths and the presence of adsorbents. XANES is the part of the absorption spectrum ranging from the absorption edge to about 40 eV above the edge. The near-edge structure is determined by the density of states available to the excited photoelectron. The coordination geometry and oxidation state affect this part of the spectrum. It is widely used in surface science and has also been used to study polymers and magnetic materials. Much chemical information can be extracted from the XANES region: formal valence (very difficult to experimentally determine in a nondestructive way); coordination environment (e.g., octahedral, tetrahedral coordination) and subtle geometrical distortions of it.

The fundamental phenomenon underlying XANES is the absorption of an X-ray photon by a core level of an atom in a solid and the consequent emission of a photoelectron (figure 1.13). The resulting core hole is filled either via an Auger process or by capture of an electron from another shell followed by emission of a fluorescent photon. The difference between XANES and traditional photoemission experiments is that in photoemission, the initial photoelectron itself is measured, while in XANES the fluorescent photon or Auger electron or an inelastically scattered photoelectron may also be measured. The distinction sounds trivial but is actually significant: in photoemission the final state of the emitted electron captured in the detector must be an extended, free-electron state. By contrast in XANES the final

state of the photoelectron may be a bound state such as an exciton since the photoelectron itself need not be detected. The effect of measuring fluorescent photons, Auger electrons, and directly emitted electrons is to sum over all possible final states of the photoelectrons, meaning that what XANES measures is the total joint density of states of the initial core level with all final states, consistent with conservation rules. The distinction is critical because in spectroscopy final states are more susceptible to many-body effects than initial states, meaning that XANES spectra are more easily calculable than photoemission spectra. Due to the summation over final states, various sum rules are helpful in the interpretation of XANES spectra.

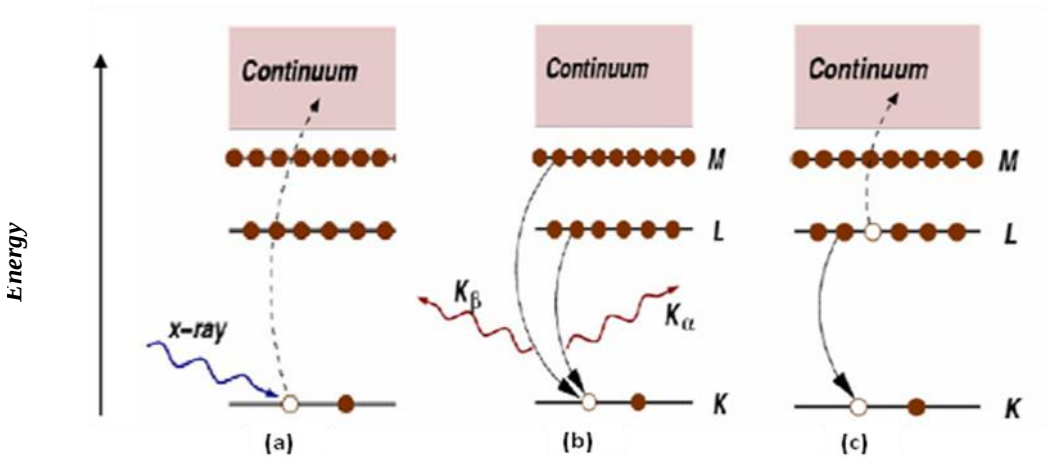

Figure 1-13 The fundamental processes which contribute to XANES spectra (a) photo absorption of an X-ray into a core level followed by photoelectron emission, followed by either (b) filling of the core hole by an electron in another level, accompanied by fluorescence; or (c) filling of the core hole by an electron in another level followed by emission of an Auger electron.

Synchrotron radiation has a natural polarization that can be utilized to great advantage in XANES studies. The commonly studied molecular adsorbents have σ and π bonds that may have a particular orientation on a surface. The angle dependence of the X-ray absorption tracks the orientation of resonant bonds due to dipole selection rules. XANES spectra are usually measured either through the fluorescent yield, in which emitted photons are monitored, or total electron yield, in which the sample is connected to ground through an ammeter and the neutralization current is monitored. Because XANES measurements require an intense tunable source of soft X-rays, they are performed at synchrotrons. Because XANES soft X-rays are

absorbed by air, the synchrotron radiation travels from the ring in an evacuated beam-line to the end-station where the specimen to be studied is mounted. Specialized beam-lines intended for XANES studies often have additional capabilities such as heating a sample or exposing it to a dose of reactive gas. The absorption peaks of XANES spectra are determined by multiple scattering resonances of the photoelectron excited at the atomic absorption site and scattered by neighbor atoms. The local character of the final states is determined by the short photoelectron mean free path, that is strongly reduced (down to about 0.3 nm at 50 eV) in this energy range because of inelastic scattering of the photoelectron by electron-hole excitations and collective electronic oscillations of the valence electrons called plasmons.

1.7.1 Chemical shift (Edge shift)

(a) Shift in the position of the main edge

The shift of the X-ray absorption edge due to chemical combination has been shown to depend primarily on the valency of the element[14]. The edge shift in general shows a marked increase with increase in oxidation state. The edge position moves towards high energy side, when the electronegativity of the ligand increases[15]. Stelling observed that in case of sulpher the edge shifted by about 0.46% in going from S^{2-} to S^{+6} complexes[16].

Boehm et al.[17] used the valancy effect to show that the cobalt in vitamin B_{12} is trivalent. Mande et al.[18] have also shown, by comparision with K-edge shifts in well known Co (II) and Co (III) compounds that freshly prepared Co (II) thiomalic acid complex is oxidised to Co (III) in air. The energy difference between the K-edge for Co (II) and Co (III) ~ 4 eV, is in agreement with the values observed by Agrawal et al.[19] and by Nigam et al.[20], the latter involved the sulphur ligand complexes. The divalency of copper in the spinal $CuMn_2O_4$ and Cu_3 $[Fe(CN)_6]$ have been established by Miller et al.[21] and by Verma et al.[22] respectively. The dependence of K-edge shifts

[14] Bergengren J., 1920, Z. Phys., **3**, 247.
Lindh A.E., 1921, Z. Phys., **6**, 303.
[15] Shulman R.G., Yafet Y., Eisenberger P. and Blumberg W.E., 1976, Proc. Nat. Acad. Sci. USA, **73**, 1384.
[16] Stelling O., 1930, Z. Phys. Chem., **7**, 210.
[17] Boehm G., Faesster A. and Riuttmayer G., 1954, Z. Naturforsch., **96**, 509.
[18] Mande C. and A.R. Chetal., 1966, *Int. Conf. X-ray Spectra and Chemical Binding*, Karl Marx Univ., Leipzig, 194.
[19] Agrawal R. M. and Nigam A. N., 1966, Proc. Ind. Acad. Sci., **63**, 200.
[20] Nigam H. L. and Shrivastava U.C., 1971 (a), Z. Naturforsch B, **266**, 997.
[21] Miller A., 1966, Phys.Chem. Solids, **29**, 633.
[22] Verma L. P. and Agrawal B. K., 1968, J Phys., **C1**, 1658.

on valence state has also been confirmed by Shrivastava et al.[23] in their experimental studies on X-ray K-edge shifts of Cu(I), Cu(II), Cu(III), Co(II), Co(III) complexes.

Sapre et al.[24] have attempted to correlate edge shift with effective charge on the absorbing atom. They have found that the edge shift towards higher or lower energy side relative to metal edge depending upon whether the absorbing atom bears the positive or negative charge. An empirical relation based on the concept of effective ionic charge has been proposed by Ghatikar et al.[25] (1978). They have also studied K-absorption spectra in ternary and complex systems[26]. They have proposed the following equation between chemical shift ΔE and the effective ionic charge q

$$\Delta E = c_1 + c_2 q \qquad (1.3)$$

where c_1 and c_2 are constants.

(b) Shift in the position of principal absorption maximum

Valancy change has been inferred from the shift in the position of the principal absorption maximum A. Vainshtein et al.[27] observed that an increase in the valency of Mn in the order $MnO \rightarrow Mn_2O_3 \rightarrow MnO_2$ resulted in a systemetic shift of the principal absorption maximum towards higher energy in agreement with Coster et al.[28]. This effect is also exhibited by the oxides and acetyl acetonates of manganese, iron and cobalt and has been related to the shift in the position of the antibonding orbitals[29]. However, the results for ferro- and ferricynides show an insignificant difference in energy. This appears to be consistent with Van Nordstrands's view that "the normal valency of the absorbing atom has an influence on the K-edge fine structure of transition metals in some cases (e q. MnO_4^- , MnO_4^{-2}, Mn-accetyl acetonates) while it has no influence in others (e. q. hexacyanides of fe)". Nigam et al.[30] have also found that the main peak for Cu(I)-thiovanol complex appears at an appreciabbly longer wavelength than those due to Cu(II) complexes. Bhide et al.[31] have shown that the absorption maximum of the Yittrium K-edge in Y^{3+}(aq) is due to the excitaiton of a 1s electron into the 5p level, the theoretial 1s→5p energy difference of 4.139×10^{18} cps agreeing well with the observed value of 4.13×10^{18} cps.

[23] Shrivastava U. C., and Nigam H. L. and Vishnoi A. N., 1972, Ind. J. Pure Appl. Phys., **10**, 61.
[24] Sapre V.B. and Mande C., 1972, J. Phys. C, **5**, 793.
[25] Ghatikar M. N. and Padalia B. D., 1978, J. Phys. C, **11**, 1941.
[26] Ghatikar M. N., Padalia B. D. and Nayak R. M., 1977, J. Phys. C, **10**, 4173
[27] Vaishtein E., Ovrutskaya R. M., Kotlyar B. I. and Linde V. R., 1974, Sov. Phys. Solid State, **5**, 2150.
[28] Coster, D. and Kiestra S., 1948, Physica, **14**, 175
[29] Glen G.L. and Dodd C.G., 1968, J. Appl. Phys., **39**, 5372.
[30] Nigam H. L. and Shrivastava U.C., 1971 (a), Z. Naturforsch B, **266**, 997.
[31] Bhide V. G. and Bhat N. V., 1963, J. Chem. Phys., **48**, 3103.

Mande et al.[32], have concluded that the K-absorption maximum in case of an octahedral complex of the first transition series corresponds to the transition 1s→4p (t_{1u}^{*}).

The totality of the edge shift data indicates a prominent role of many other factors besides the metal oxidation state[33]. Thus, the residual charge on the metal ion, ionic covalent character of the metal-ligand bond, the presence of the electronegativity and polarisablity of the ligand play a decisive role in the final analysis of the K-absorption spectra.

1.7.2 Edge structure

(a) Edge-width and co-ordination stoichiometry

Edge-width can be defined as the difference of the energy between the inflection point of the absorption edge K and the principal absorption peak A.. According to Cauchois[34], the difference in frequency between the absorption discontinuity and the principal absorption maximum should increase with the atomic number, exception being her own results on nickel, copper, zinc and zirconium in their saturated salt solutions.

An empirical correlation between edge-width E_w of the metal and co-ordination stoichiometry have been proposed by Nigam et al.[35] The relation is given by the equation

$$[E_w \sum (X_M - X_L)]^{1/2} = \text{constant} \qquad (1.4)$$

where X_M and X_L are the Pauling electronegativities of the central metal and nearest neighbour respectively. The above empirical relation has been verified by utilizing the data of a number of workers[36], It is important to mention here that the predictability of coordination stoichiometry from edge-width data requires some refinement in order to be more rigorous. Since the electronegativity of an element depends upon the valence

[32] Mande C. and A.R. Chetal., 1966, *Int. Conf. X-ray Spectra and Chemical Binding*, Karl Marx Univ., Leipzig, 194.
Sinha K. P. and Mande C., 1963, Ind. J. Phys., **37**, 257.
[33] Kumar A., Nigam A. N. and Shrivastava B. D., 1981, X-ray Spectrom., **10**, 25
[34] Cauchois Y., 1948, C. R. Acad. Sci., **227**, 65.
[35] Nigam H.L. and U.C.Srivastava, 1971(b), Chem. Commum., **14**, 761.
[36] Deodhar G. B., 1966, *Int. Conf. on X-ray spectra and chemical binding*, Karl Max Univ., Leipzig, 65.
Awasthi P. K., 1981, *Ph. D. Thesis*, Vikram University, Ujjain.
Shrivastava U.C. and Nigam H.L., 1971, Ind. J. Pure Appl. Phys., **9**, 1301.
Prasad J., Krishna V. and Nigam H. L., 1976, J. Chem. Soc., Dalton, 2413.
Prasad J., Krishna V. and Nigam H. L., 1977, J. Phys. Chem. Solids., **38**, 149.
Krishnan V., Prasad J. and Nigam H.L., 1976, Inorg. Chem. Acta **20**,193.
Bhargava C. B., Vishnoi A. N. and Shrivastava U. C., 1978, Indian J. Chem., **16** A,

state, the chemical environment etc. of the element and therefore the group electronegativity of the molecule should be considered, which may perhaps give more reliable information about the coordination stoichiometry of a complex using relation (1.4).

(b) Edge structure and stereochemistry

The variation in intensity in the different regions of the K-absorption edge, which gives rise to a characteristic shape of the absorption coefficient curve, have been correlated with many stereochemical features of a coordination complex. The product of transition probablity and the density of state give the X-ray intensity. The density of state depends upon the nature, number and symmetry of nearest neighbors. Thus, according to Jorgensen[37], in an octahedral complex of a 3d metal, the only possible Laporte allowded and symmetry allowded transitions are from 1s to 4p orbitals. Bhide et al[38]. used the results of Mossbauer spectra to discuss the edge structure of some yittrium complexes. A number of attempts have been made to apply the molecular orbitals (MO) theory for interpreting the features of K-absorption edge[39] have systematically developed the application of the MO theory to interpret the main features of the structure of the K-absorption edge for a good number of coordination complexes involving first transition metals.

The most relevant features to study the stereochemistry of a complex are

(i) The shape of the edge

(ii) Low energy absorption

(iii) Splitting or broadening of the main peak.

(i) Shape of the edge

It has been found that the shape of the absorption edge, which is determined by the relative intensities and widths of the low-lying 'bound state' transitions, reveals details of the geometry of the metal complex and the number and nature of the surrounding ligands[40]. The principle features of absorption spectra have been

---

[37] Jorgensen C. K., 1962, Solid state phys., **13**, 448.

[38] Bhide V. G. and Bhat N. V., 1963, J. Chem. Phys., **48**, 3103.

[39] Prasad J., Krishna V. and Nigam H. L., 1976, J. Chem. Soc., Dalton, 2413.

[39] Prasad J., Krishna V. and Nigam H. L., 1977, J. Phys. Chem. Solids., **38**, 149.
Obashi M., 1978, Jpn. J. Applied Phys., **17**, 563.
Sarode P. R. and Pendharkar A. V., 1978, Chem. Phys., **28**, 455.
Glen G.L. and Dodd C.G., 1968, J. Appl. Phys., **39**, 5372.
Seka N. and Hason H. P., 1969, J Chem. Phys., **50**, 344.

[40] Cramer S.P., 1977, *Ph. D. Thesis*, Stanford Univ.
Hu V. H., Chan S. I. and Brown G. S., 1977, Proc. Natl. Sci. USA **74**, 3821.

explained by many workers[41] on the basis of ligand field theory. The arc-tangent shape of the absorption edge was first described by Ritchmeyer[42] et al. The position of X-ray absorption edge depends, for example, on the valency of the absorbing ion, the effective nuclear charge (ENC) on the central atom[43] and also upon the geometry of the complexes etc[44].

(ii) Low energy absorption

The low energy absorption can be defined as a feature that may appear with enhanced in intensity due to a mixing of s, p, d-character in the orbitals. In case of transition metal complexes, having empty low energy d-orbitals, the low energy absorption is assigned as 1s→nd. Vainshtein et al[45]. observed two small maxims in the 1s →3d region, attributable to the splitting of the 3d orbitals into 3d t_{2g} and 3d $e_{g'}$ under the influence of the crystal field due to surrounding O^{2-} ions. Such a splitting has also been observed by Nigam et al[46]. in the case of cobalt-thiopropinic acid and cobalt thiovanol complexes. Gusatinskii et al[47] have shown that the initial region of the absorption spectrum (lower region of wavelength) depends upon the character of the first coordination polyhedron of the absorbing atom. According to Mitchell et al.[48], the expectation of the X-ray K-absorption region for planar and tetrahedral symmetry involving sd^3 bonding in some covalent complexes of chromium, manganese, iron and nickel have been confirmed by experiments. Mande et al.[49] have determined the coordination number and symmetry in the hydrated and anhydrous oxinate complexes of cobalt and also in the pink and blue cobalt chloride solution.

---

[41] Sinha K.P. and Mande C., 1963, Ind. J. Phys., **37**, 257.
Mande C. and A.R. Chetal., 1966, *Int. Conf. X-ray Spectra and Chemical Binding*, Karl Marx Univ., Leipzig, 194.
Padalia B. D. and Krishnan V., 1971, J. Pure and Appl. Phys., **9**, 813.

[42] Ritchmeyer F. K. and Barnes S. W., 1934, Phys. Rev., **46**, 843.

[43] Becker M. V., 1964, Naturwissenschaften, **51**, 633.
Ovsyannikova J. A., Batsanova S. S., Nosonova L. I., Batsanova L. R. and Nakrasova E. A., 1967, Bull. Acad. Sci. USSR, **8**, 805.
Barinskii R. L., 1967, J. Struct. Chem.USSR, **8**, 805.

[44] Heintz D., 1969, *Dissertation*, Munich University.
Meisel A., 1965, Phys. Status Solidi., **10**, 365.

[45] Vainstein E. E., Shurakwasni E. A. and Stari I. B., 1959, Zh. Neorg. Khim., **4**, 881.

[46] Nigam H. L. and Shrivastava U.C., 1971 (a), Z. Naturforsch B, **266**, 997.

[47] Gusattinskii A. N. and Ischenoko S.A., 1967, Acad. Sci. USSR Phys. Ser., **31**, 1017.

[48] Mitchell G. and Beeman W. E., 1952, J. Chem. Phys., **20**, 1298.

[49] Mande C. and Chetal A. R., 1964(a), Indian J. Phys., **38**, 433.
Mande C. and Chetal A. R., 1964(b), Curr. Sci., **33**, 707.

(iii) Splitting of the main peak

It is generally recognised[50] that the splitting of the K-absorption peak for compounds of the 3d-transition series metals is a manifestation of the splitting of the otherwise triply degenerate $4p^*$ antibonding molecular orbitals under the influence of the field due to surrounding ligands. A quantum mechnical analysis of the symmetry dependence of the crystal field splitting of p-orbitals generated by Cotton et al.[51], has shown that the degenerate p-level, and hence, the absorption peak, remains unsplit in a regular octahedral (oh) field, while it splits into two or more components as the coordination symmetry is lowered. These conclusions have been supported experimentally by a number of workers[52] in several compounds, certain ligands seem to cause splitting or broadening irrespective of symmetry considerations.

1.7.3 Applications of XANES spectroscopy

Much chemical information can be extracted from the XANES region: formal valence (very difficult to experimentally determine in a nondestructive way); coordination environment (e.g., octahedral, tetrahedral coordination) and subtle geometrical distortions of it. Transitions to bound vacant states just above the Fermi level can be seen. Thus XANES spectra can be used as a probe of the unoccupied band structure of a material. The near-edge structure is characteristic of an environment and valence state hence one of its more common uses is in fingerprinting: if you have a mixture of sites/compounds in a sample you can fit the measured spectra with linear combinations of XANES spectra of known species and determine the proportion of each site/compound in the sample.

1.8 Extended X-ray absorption fine structure

In X-ray absorption spectra, the absorbed photon ejects a core photoelectron from the absorbing atom, leaving behind a core hole. The atom with the core hole is now

[50] Glen G.L. and Dodd C.G., 1968, J. Appl. Phys., **39**, 5372.
Kauer I., 1956, Z. Phys. Chem., **6**, 105.

[51] Cotton F. A. and Ball Hausen C. J., 1956, J. Chem. Soc., **25**, 617.

[52] Kauer I., 1956, Z. Phys. Chem., **6**, 105.
Obashi M., 1978, Jpn. J. Applied Phys., **17**, 563.
Glen G.L. and Dodd C.G., 1968, J. Appl. Phys., **39**, 5372.
Cotton F. A. and Ball Hausen C. J., 1956, J. Chem. Soc., **25**, 617.
Cotton F. A. and Hanson H. P., 1958, J. Chem. Phys., **28**, 83.

excited. The ejected photoelectron's energy will be equal to that of the absorbed photon minus the binding energy of the initial core state. The ejected photoelectron interacts with electrons in the surrounding non-excited atoms.

If the ejected photoelectron is taken to have a wave-like nature and the surrounding atoms are described as point scatterers, it is possible to imagine the backscattered electron waves interfering with the forward-propagating waves. The resulting interference pattern shows up as a modulation of the measured absorption coefficient, thereby causing the oscillation in the EXAFS spectra. A simplified plane-wave single-scattering theory has been used for interpretation of EXAFS spectra for many years, although modern methods (like FEFF, GNXAS) have shown that curved-wave corrections and multiple-scattering effects cannot be neglected. The photoelectron scattering amplitude in the low energy range (5-200 eV) of the photoelectron kinetic energy becomes much larger so that multiple scattering events become dominant in the NEXAFS (or XANES) spectra.

The wavelength of the photoelectron is dependent on the energy and phase of the backscattered wave which exists at the central atom. The wavelength changes as a function of the energy of the incoming photon. The phase and amplitude of the backscattered wave are dependent on the type of atom doing the backscattering and the distance of the backscattering atom from the central atom. The dependence of the scattering on atomic species makes it possible to obtain information pertaining to the chemical coordination environment of the original absorbing (centrally excited) atom by analyzing these EXAFS data.

EXAFS spectroscopy provides structural information about a sample by way of the analysis of its X-ray absorption spectrum. It allows determining the chemical environment of a single element in terms of the number and type of its neighbors, inter-atomic distances and structural disorders. This determination is confined to a distance given by the mean free path of the photoelectron in the condensed matter, which is between 5 and 10 Å radius from the element[53]. These characteristics make EXAFS a powerful structural local probe, which does not require a long-range order. It is an important technique in several fields of natural sciences, from earth sciences to biochemistry. Since EXAFS is a technique selective for a particular element and

[53] Koningsberger D. C. and Prins R., 1988, *X-Ray Absorption: Principles, Applications, Techniques of EXAFS, SEXAFS and XANES; Chemical Analysis,* Volume 92, (John Wiley and Sons, New York).
Teo B. K., 1986, *EXAFS: Basic Principles and Data Analysis*, Inorganic Chemistry Concepts, Vol. 9 (Springer-Verlag, Berlin).
Fornasini P., *Introduction to X-ray absorption spectroscopy,* 2003, in: S. Mobilio and G. Vlaic (Eds.) *Synchrotron Radiation: Fundamentals, Methodologies and Applications,* Conference Proceedings, Vol. 82, SIF, Bologna, pp. 129–170.

sensible only for a short-range order, it is one of the most appropriate spectroscopy to be applied in the cases of amorphous solids, e.g., ceramics, liquids, e.g., solutions of ionic compounds or gels which cannot be studied by X-ray diffraction, biomolecules, e.g., solutions of metalloproteins, and homogeneous and heterogeneous catalysts.

Furthermore, EXAFS does not require any particular experimental conditions, such as vacuum (at least in principle). There are several types of sample-holders that allow collecting experimental data under varying temperature and pressure, or while the sample is undergoing a chemical reaction[54] (in-situ studies). Measures taken under working conditions are of critical importance in the case of heterogeneous catalysts in order to understand their behavior during catalysis, and in studying temperature and pressure induced changes. On the other hand, there are some problems associated with this spectroscopy. First, the necessity of synchrotron light as a source, which is expensive and not easily available. Second, the use of simulation and best-fit procedures to obtain structural parameters; these methods are time consuming and they sometimes give ambiguous or unreliable results. However, if the system under study is properly chosen, EXAFS is able to supply useful and even essential information.

1.8.1 Origin of the EXAFS signal

The X-ray absorption coefficient for an atom, indicated as μx, is directly proportional to the probability of absorption of one photon and is a monotone decreasing function of energy. It shows several discontinuities known as absorption edges: they occur when the energy of the incident photons equals the binding energy of one electron of the atom and are classified with capital letters (K, L, M...) according to the principal quantum number of the electron in the ground state (n = 1, 2, 3...).

The edge energy is characteristic of each atom. In the case of an isolated atom (monatomic gas), the absorption coefficient decreases monotonously with energy between two subsequent edges. In all other situations, the spectrum also shows oscillations that start at the edge and finish a thousand eV above. An incident photon is able to extract a core electron if its energy is equal to or greater than the edge

[54] Van Bokhoven J. A., Van Bokhoven, A. M., Eerden J. V., Smith A. D. and Koningsberger D. C., 1999, J. Synch. Rad., **6,** 1120.

energy. The ejected electron is called photoelectron and it has the characteristics of both a particle and a wave. Its kinetic energy is given by:

$$E = E_x - E_0 \tag{1.5}$$

where E_x is the energy of the X-ray photon and E_0 the energy of the edge. Its wave vector modulus is given by:

$$|k| = \frac{2\pi}{\lambda} = \sqrt{\frac{8\pi^2 m}{h^2}(E_x - E_0)} = \sqrt{0.263 \times E} \tag{1.6}$$

If the absorbing atom is isolated in space, the photoelectron propagates as an unperturbed isotropic wave (fig.1.14A), but in most cases there are many other atoms around the absorber. These become scattering centers of the photoelectron wave (fig. 1.14B). The final state of the photoelectron can be described by the sum of the original and scattered waves. This leads to an interference phenomenon that modifies the interaction probability between core electrons and incident photons. Constructive interference increases while destructive interference decreases the absorption coefficient of the atom. This interference phenomenon, for a given energy of the photoelectron, depends on the distance between emitting and scattering atoms, and their atomic numbers. The EXAFS signal $\chi(k)$ is defined as a function of the wave vector k by eqn. (1.2).

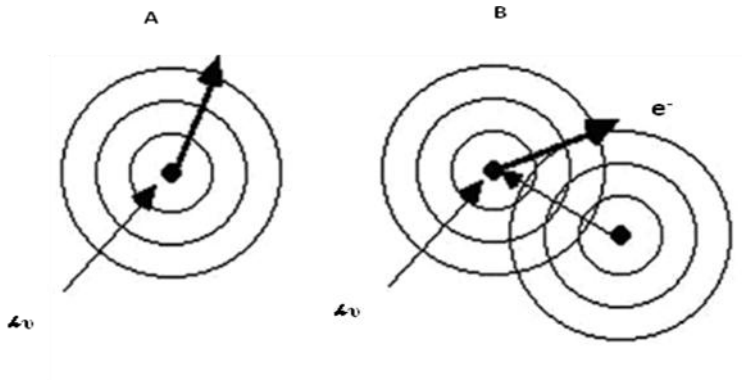

Figure 1-14 (A) & (B) Schemes of scattering processes.

1.8.2 Early history of EXAFS

A fine structure beyond an absorption edge was first observed about 80 years ago[55]. However, it took more than 40 years to interpret this phenomenon and to realize that accurate, detailed, structural information could be extracted from it. Early progress was impeded by experimental limitations of the then available X-ray sources[56]. Moreover, the theoretical interpretation was also not clear cut at that time. This is not surprising, since a full treatment turns out to depend on many complicated details of atomic and molecular structure, high-energy electron-atom scattering, many-electron processes, vibrational structure and disorder. Indeed, much of this physics has only been unraveled within the past 30 years, and a fully quantitative theory was not developed until the present decade. Kronig[57] (1931) was the first who attempted to explain EXAFS by the long-range order in a system. Later, this mechanism broke down. One year later, Kronig (1932) proposed another theory, which was based on the substantial importance of short-range order and attributed EXAFS to the modulation of the final-state wave function of a photoelectron scattered on the neighboring atoms. This approach was later further developed[58] and provides the basis of the current concept of the EXAFS.

In Kronig's theory, the oscillatory structure in EXAFS was attributed to the influence of neighboring atoms on the transition matrix element in the golden rule, i.e., a short range-order effect (Kronig, 1932). This type of theory is most often used today to explain the origin of EXAFS, although, as we shall see later, both long and short range-order theories can be reconciled when appropriate broadening is

---

[55] Fricke, H., 1920, Phys. Rev., **16**, 202.
Hertz G., 1920, Z. Phys., **3**, 19.
Coster, D., 1924, Z. Phys., **25**, 83
Lindh A.E., 1925, Z. Phys., **31**, 210.
Kievit B. and Lindsay G.A., 1930, Phys. Rev., **36**, 648.
Hanawalt J.D., 1931, Z. Phys. **70**, 20; 1931, Phys. Rev., **37**, 715.
Ray B.B., 1929, Z. Phys., **55**, 119.

[56] Stumm von Bordwehr, R., 1989, Ann. Phys. (Paris), **14**, 377.
Lytle, F. W., 1999, J. Synchrotron Radiat., **6**, 123.

[57] Kronig R., 1931, Z. Phys., **70**, 317.
Kronig R., 1932, Z. Phys., **75**, 468.

[58] Peterson H., 1932, Z. Phys., **76**, 768.
Kostarev A.I., 1941, Zh. Eksp. Teor. Fiz. **11**, 60; 1949, Zh. Eksp. Teor. Fiz., **19**, 413.
Kozlenkov A.I., 1961, Izv. Akad. Nauk SSSR, Ser. Fiz., **25**, 957.
Sawada M., 1959, Rep. Sci. Works Osaka Univ., **7**, 1.
Shmidt, V. V., 1963, Izv. Akad. Nauk SSSR, Ser. Fiz., vol. 27, p. 392.

introduced. The short-range-order theory reflects the quantum mechanical wavelike nature of the final, excited, photoelectron state. That is, the dominant wiggles in the EXAFS spectrum are interpreted as a quantum interference phenomenon. The outgoing photoelectron can be viewed as a quantum wave that spreads out over the solid, much as a rock thrown in a pond creates an expanding spherical wave in water. In the same way that water waves reflect off of any obstacles in the pond and, in turn, reflect other waves back toward the original point of the splash, so other atoms will reflect the electron wave back towards the original atom. The topmost atom is the original source of the wave, which diffracts first off the atom at the lower left and finally off the atom at the lower right. Each successive outgoing spherical wave is weaker, which is reflected in the thickness of the spherical wave fronts. This type of path is called a triangular path.

The amplitude of all the reflected electron waves at the absorbing atom add either constructively or destructively to the outgoing photoelectron wave and hence modulate the matrix element between the initial and final states that controls the strength of the transition. Because this interference pattern changes with the energy of the photoelectron (note that the de Broglie wavelength λ of the electron wave varies inversely with the wave vector k or momentum of the electron), the matrix element, and consequently the absorption, will exhibit similar oscillations. The modern resolution to the controversy between the short and long-range-order approaches lies in the energy-dependent competition between scattering strength and inelastic losses. A crucial element is the recognition that a high-energy, excited photoelectron state is not infinitely long lived, but must decay as a function of time and distance and hence cannot probe long-range effects. This decay is due primarily to inelastic losses (i.e., ‘‘extrinsic losses’’) as it traverses the material, either by interacting with and exciting other electrons in the solid, or by creating collective excitations (e.g., losing energy to plasmon production). In addition, the intrinsic lifetime of the core-hole state (i.e., ‘‘intrinsic losses’’) must be considered. In phenomenological terms, the original outgoing wave of the excited photoelectron dies away as it moves further away from the absorbing atom. Ultimately it becomes too weak to significantly reflect any waves off of distant atoms. The returning reflected waves also suffer this same type of extinction. The net effect is that EXAFS can only measure the local atomic structure over a range limited by the net lifetime (or effective mean free path) of the excited photoelectron. This range is typically on the order of tens of angstroms or an inverse

lifetime of a few eV and roughly follows a universal dependence[59]. The short-range-order theory focuses on this short-range interference between several important scattering paths.

1.8.3 Analytical expression of the EXAFS signal

In order to extract structural information from experimental spectra, a simple analytical expression that relates the EXAFS signal to the structural parameters is required. To obtain a simplified EXAFS formula we must accept some approximations. First of all, the dipole approximation, which describes well the interactions between core electrons and hard X-ray photons. This approximation allows writing the absorption cross-section as:

$$P_{if} = \frac{2\pi^2 e^2}{m^2 \omega} |M_{if}|^2 \rho(E_f) \qquad (1.7)$$

where i and f stand for initial and final states of the electron, e and m are its charge and mass, $\rho(E_f)$ is the state density available to the electron (it is considered as a free electron so there is a continuous distribution of states), ω is the incident photon frequency and $|M_{if}|$ is a dipole matrix element related to the transition of the electron from i to f state.

$$|M_{if}| = \langle \psi_f | p.e | \psi_i \rangle \qquad (1.8)$$

where p is the momentum operator, e is the electric field vector of the X-ray photon, Ψ_i and Ψ_f are wave functions for i and f states.

The hard part of the job is to obtain a good expression of the final state wave function. This can be done by choosing a proper approximation for the potential function that describes the system. In most cases this is solved using the muffin-tin approximation. Moreover, the single electron approximation and the sudden approximation are introduced. Under these conditions, Ψ_f depends on the absorbed photon energy and can be written as a linear combination of two terms: the wave function for the photoelectron outgoing the excited atom Ψ_{out} and a perturbing term Ψ_{sc} which represents the backscattered wave.

[59] Seah M. P., and Dench W. A., 1979, Surf. Interface Anal., **1**, 2.

At this point, keeping in mind that the absorption coefficient is proportional to P_{if}, it is possible to write a theoretical expression of the EXAFS signal:

$$\chi(k) = \frac{\langle \psi_{out} + \psi_{sc} | p.e | \psi_i \rangle}{\langle \psi_{out} | p.e | \psi_i \rangle} - 1 \qquad (1.9)$$

Starting from this formula and with several mathematical transformations and minor physical approximations, it is possible to write an EXAFS analytical expression like the one suggested by Kelly (2008):

$$\chi(k) = \sum_j \frac{N_j S_0^2 F_j(k)}{kR_j^2} \times \exp(-2\sigma_j{}^2 k^2) \times \exp\left(-2R_j / \lambda(k)\right) \times \sin[2kR_j + \delta_j(k)] \qquad (1.10)$$

$$\text{with} \quad R_j = R_{0j} + \Delta R_j \quad \text{and} \qquad k^2 = \frac{2m_e(E - E_0 + \Delta E_0)}{\hbar}$$

In this equation, k is the wave vector modulus for the photoelectron; The term R_j is the half path length of the photoelectron (i.e. the distance between the absorber and a coordinating atom for a single-scattering event). The value of R_{0j} is the half path length used in ther theoretical calculation which can be modified by ΔR_j. Kelly (2008) has defined each of the terms of this equation in detail and the same is being reproduced below:

(1) (N_j S_0^2): These terms modify the amplitude of the EXAFS signal and do not have a k-dependence. The subscript j indicates that this value can be different for each path of the photoelectron. For single scattering, N_j represents the number of coordinating atoms within a particular shell. For multiple scattering, N_j represents the number of identical paths. The passive electron reduction factor (S_0^2) usually has a value between 0.7 and 1.0 (Li et al., 1995). S_0^2 accounts for the slight relaxation of the remaining electrons in the presence of the core hole vacated by the photoelectron. S_0^2 is different for different elements, but the value is generally transferable between different species from the same element and the same edge.

(2) $F_j(k)$: This term is the effective scattering amplitude. For a single scattering path it is the atomic scattering factor used in X-ray diffraction. For a multiple scattering path it is an effective scattering amplitude written in terms of the single scattering

formalism (Rehr and Albers, 1990). This term accounts for the element sensitivity of EXAFS. In general, atoms with more electrons scatter photoelectrons more strongly at higher wavenumbers. Because $F_j(k)$ depends on the number of electrons, it is similar between elements with nearly the same number of electrons. The EXAFS signal from elements separated by only one atomic number on the periodic table such as O, N, and C can rarely be distinguished on the basis of their scattering amplitude alone.

(3) $\mathbf{1/R_j^2}$**:** The contribution from a shell of atoms ar a distance R_j diminishes with incresing distance from the absorber.

(4) $\mathbf{exp(-2\sigma_i^2k^2)}$**:** Because all of the coordinating atoms in a shell are not fixed at positions of exactly a distance R_i from the central absorber atom, s2 accounts for the disorder in the interatomic distances. σ^2 is the mean-square displacement of the bond length between the absorber atom and the coordination atoms in a shell. This term has contributions from dynamic (thermal) disorder as well as static disorder (structural heterogeneity). A distribution of distances within a single shell decreases the amplitude of the EXAFS signal because the phase differences between outgoing and scattered photoelectrons are shifted slightly for each atom in the coordination shell. The EXAFS process occurs on the femto-second (10^{-15} s) time scale, while thermal vibrations occur on a much longer time scale of 10^{-10} to 10^{-12} s. Because the atoms are essentially "frozen" at one position about their thermodynamic minima during the excitation process, EXAFS spectra measure the distribution of the distances between the absorber atom and each of the coordinating atoms within a shell in terms of a σ^2 value. The static disorder component of σ^2 is due to differences in the position of the minima themselves. Thus, for example, if two interatomic distances are separated by only 0.010 Å, with one atom at 2.00 Å and another atom at 2.10 Å, the contributing EXAFS signal could be modeled with one scattering path at 2.05 Å with a mean disorder of 0.05 Å such that there is an additional σ^2 term due to the static disorder of 0.0025 $Å^2$.

(5) $\mathbf{exp\left(-2R_j/\lambda(k)\right)}$**:** This exponential term depends on $\lambda(k)$, the mean free path of the photoelectron, which is the mean distance that a photoelectron travels after

excitation. The mean free path of a photoelectron decreases from approximately 15 Å for short wavenumbers of 1 $Å^{-1}$, goes through a minimum of 5 Å for wavenumber of 2.5 $Å^{-1}$, and then increases to 30 Å for large wavenumbers of 15 $Å^{-1}$. It is this term that causes the EXAFS signal to be dominated by the scattering contributions from atoms within approximately 10 Å of the absorber atom and makes EXAFS a local structural probe.

(6) $\sin[2kR_i + \delta_i(k)]$: This term accounts for the oscillations in the EXAFS signal with a phase given by $2kR_i + \delta_i(k)$. The path of the photoelectron is described by $2R_i$ (the distance to the neighboring atom and then back to the absorber atom), which is multiplied by its wavenumber (k) to determine the phase. $\delta_i(k)$ is a phase shift of the photoelectron caused by the interaction of the photoelectron with the nuclei of the absorber atom and the interaction with the nuclei of the coordinating atoms of the photoelectron path. Because the photoelectron has a negative charge and the nucleus is positively charged, the photoelectron loses energy and its wavelength lengthens as it interacts with the coordinating atoms and the absorber atom. It is this sine term in the EXAFS equation that makes the Fourier transform (FT) of the XAFS signal such a powerful tool, because a FT results in peaks at distances related to R_i, the interatomic distances between the absorber and coordinating atoms. The peak is not precisely at R_i due to the phase shift $\delta_i(k)$, which causes a shift in distance of approximately −0.5 Å.

(7) ΔR_i: This term reprents a change to the interatomic distance relative to the initial path length R_i. The path length can be changed slightly (>0.1 Å) to optimize the model to the data.

(8) ΔE_i: This term relates to a change in the photoelectron energy. This value is used to align the energy scale of the theoretical spectrum to match the measured spectrum.

Eqn. (1.10) is valid in the case of non-oriented samples (crystalline powders, solutions and gases) and/or in the case of a non-polarized light source. Using polarized light, like synchrotron radiation, with monocrystals implies a correction of the equation: it must be multiplied by 3 $\cos^2\theta$ where θ is the angle between the

absorber-scatterer axis and the polarization direction. Non-oriented samples do not require this correction, because the angle is isotropically distributed in space. Eqn. (1.10) is able to describe only single scattering processes. However, it has been demonstrated that considering also multiple scattering processes leads to a very similar analytical expression. Introducing multiple scattering allows one to obtain also stereo-chemical information about the local structure[60] (Filipponi, 1995).

1.9 EXAFS data analysis

The basic scheme for EXAFS data analysis was outlined in early 1970s by Stern, Lytle and Sayers[61]. Since then various refinements and extensions have been added to the original scheme. The methods of analyzing EXAFS data include Fourier transform techniques[62], the ratio method[63], maximum entropy spectral estimation, beat analysis, least squares fitting procedures in either wave number (k) or coordinate (r) space using theoretical or impirical backscattering functions (Hayes et al., 1976; Lee et al., 1981), and hybrids of these. Later it was shown that at a particular value of the energy $E_0 = E_c$ for which the peak position in the Fourier transform is independent of the weighting factor k^n, the phase shift is a linear function of k[64]. Making use of this linearity the bond length in any unknown material could be evaluated without inverse Fourier transforming the data, with the help of the known bond distance in a model compound which is chemically similar to the unknown material. The method proposed by Stern has the advantage that it provides much cleaner data for selection of single peaks for back transformation than those generated at other E_0 values, reducing the errors in EXAFS data analysis. The method for determination of bond length using Fourier transformatoin technique is furthur discussed in section 1.9.2 below.

---

[60] Filliponi A., Di Cicco A., and Natoli C. R., 1995, Phys Rev B, **52**,1.

[61] Stern E.A., 1974, Phys. Rev. B, **10** 3027.
Lytle F. W., Sayers D. E. and Stern E. A., 1975(a), Phys. Rev. B, **11,** 4825
Stern E. A., Sayers D. E. and Lytle F. W., 1975, Phys. Rev. B, **11**, 4836.

[62] Kelly S. D., Hesterberg D. and Ravel B., 2008, *Methods of Soil Analysis. Part 5. Mineralogical Methods*, (Soil Science Society of America, Madison, USA), Chapter 14.
Stern E.A., 1974, Phys. Rev. B, **10** 3027.
Lytle F. W., Sayers D. E. and Stern E. A., 1975(a), Phys. Rev. B, **11,** 4825
Stern E. A., Sayers D. E. and Lytle F. W., 1975, Phys. Rev. B, **11**, 4836

[63] Stern E. A., Sayers D. E. and Lytle F. W., 1975, Phys. Rev. B, **11**, 4836

[64] Stearns M.B., 1982, Phys.Rev.B, 25, 2383.

1.9.1 Different methods of determination of bond lengths from EXAFS data

Apart from the Fourier transformation technique mentioned below and in section 1.9.2, the bond lengths can also be determined from EXAFS data by three graphical methods. Infact before the Fourier transformation technique was formulated, the bond length used to be extracted from the EXAFS data by the three graphical methods. We have used all the three methods for determination of bond lengths in copper complexes and copper salts studied in the present thesis. The three methods are described below:

(a) Levy's method[65]

Levy has outlined a simple method of determining bond length. According to this method the bond length R_1 is given by-

$$R_1 = \left(\frac{151}{\Delta E}\right)^{1/2} \text{ Å} \qquad (1.11)$$

where ΔE is energy difference between the first EXAFS maxima B and first EXAFS minima β.

(b) Lytle's method

Lytle employed a "particle in a box" theory to calculate the bond length[66]. In this theory, a nearly spherical atomic polyhedron (wigner-Seitz unit cell) was constructed in the lattice and approximated by a sphere of equivalent volume with radius r_s. The energy states available to the ejected photoelectrons were calculated by Schrödinger equation and written as

$$E = (h^2 / 8mr_s^2)Q_{nl} \qquad (1.12)$$

where $Q = (X_{ne}\,\pi)^2$ was termed as energy level. Lytle argued that if the electron wave front has a node in the neighborhood of the surrounding atom, electron wave functions satisfy the condition of resonance. Therefore, one can identify E with the

[65] Levy R. M., 1965, J. Chem. Phys., **43**, 1846.
[66] Lytle F.W., 1966, Advances in X-ray Analysis, **9**,398

energies of absorption maxima in EXAFS. The observed E versus Q was plotted. A straight line in slope M was obtained such that-

$$R_s(\text{Å}) = \{37.60 / M\}^{\frac{1}{2}} \qquad (1.13)$$

the value of R_s gives the radius of a sphere with volume equal to the volume of the respective polyhedral.

It is noted that the value of R_s determined from E-Q plot is the radius of a sphere surrounding the absorbing atom having volume equal to that of Wigner-Seitz cell and not the interatomic distance. The later has to be derived from R_s by multiplying it with a factor greater than unity and appropriate to the geometry of the system. Lytle has shown that the factor is 1.14 for fcc structure. For hcp structure, the factor is very nearly equal to unity.

It was found that E versus Q plots pass through origin in metals, but not in compounds. Agrawal et al.[67], tried to explain it using double potential models, instead of the Lytle's single potential model.

(c) L.S.S. method

Although, Fourier transform of EXAFS data is a general and powerful technique to determine many physical parameters; however, it is possible to determine nearest-neighbur distances and phase shifts from a simple graphical technique[68]. This is possible because the first shell scattering usually dominates the EXAFS curves; then, if only the major EXAFS peaks are used, the period will be that of the first coordination shell. In this method, the energy positions of the maxima and minima in EXAFS are measured with respect to the inflection point on the main absorption edge, which signifies the Fermi level in metals and the first unoccupied level of suitable symmetry available for the absorption of the ejected electron in the case of compounds. Any error occurring in the measurements due to choice of E_0 would therefore be the same in compounds of a given system type, since measurements are made with reference to the same point on the absorption curves. Even if the value of E_0 is not taken into account (by putting $E_0 = 0$), it does not cause any serious problem

[67] Agarwal B K and Johri R K, 1977(a), J. Phys. F, **7**, 1607.
Agarwal B K and Johri R K, 1977(b), J. Phys. C, **10**, 3213.
[68] Lytle F. W., Sayers D. E. and Stern E. A., 1975(a), Phys. Rev. B, **11,** 4825.

in the EXAFS data analysis when the graphical method is used. This is a great advantage of this method over the computational method of data analysis. The expression for the wave vector *k* then reduces to

$$k = \left[\frac{2m}{h^2}E\right]^{1/2} = (0.263E)^{1/2}. \qquad (1.14)$$

In eqn. (1.10) the sine term determines the periodicity of the EXAFS function. The term $2kR_j$ indicates the phase shift as a free electron of wave vector k traverses the distance $2R_j$. Besides this, an additional phase shift $\delta_j(k) = 2\Phi_j(k)$ is added because in a solid the ejected photoelectron moves in the presence of potentials. The phase shift $\Phi_j(k)$ is made up of two contributors, one from the central atom and other from the backscattering atoms. If this factor were absent, the frequency of oscillations with respect to k would be a direct measure of R_j. However, $\Phi_j(k)$ which is k dependent also contributes to this frequency. Assuming that $\Phi_j(k)$ is linear in k, we can write

$$\Phi_j(k) = -\alpha_j k + \beta_j \qquad (1.15)$$

Substituting this value of $\Phi_j(k)$ in eqn. (1.10), one notes that the frequency of oscillation with respect to k is proportional to $(R_j - \alpha_j)$. Thus the phase $\Phi_j(k)$ contributes a shift in the determination of atomic positions and hence this shift must be determined in an appropriate manner in order to obtain precise values of R_j. The sine term thus becomes

$$\sin[2kR_j + 2(-\alpha_j k + \beta_j)]. \qquad (1.16)$$

When only the prominent absorption maxima and minima in the EXAFS are considered, it is found that the first shell scattering decides the nature of the EXAFS function. Therefore putting j = 1 for the first coordination shell scattering, and then substituting eqn. (1.16) into eqn. (1.10), it was observed[69] that the maxima and minima in $\chi(k)$ occur when

$$\frac{n\pi}{2} = 2k(R_1 - \alpha_1) + 2\beta_1 \qquad (1.17)$$

Where n is an integer. For the maxima in EXAFS, n = 0, 2, 4,…. and for the minima, n = 1, 3, 5,…. By plotting n against k, the value of $(R_1 - \alpha_1)$ can be obtained from the

[69] Lytle F. W., Sayers D. E. and Stern E. A., 1975(a), Phys. Rev. B, **11,** 4825.

slope of the curve. Knowing the value of R_1 from crystallographic data for a standard material, the value of α_1 can be obtained. Its value primarily depends upon the type of chemical bond in a material. For very similar chemical systems α_1 can be taken as constant which helps in determining the value of R_1 in materials for which it is not known. The intercept of the n versus k plot gives the value of β_1. This graphical method was used by several workers[70] for the analysis of their EXAFS data, primarily for the determination of bond lengths from the values of α_1. However the factor β_1 has not received much attention so far.

There have been continuous efforts to modify eqn. (1.10) in order to make it more general and applicable to different experimental situations. It was shown [71] that the sign of the amplitude of the EXAFS function should be chosen in such a way that the backscattering amplitude become positive. The EXAFS theory was further modified by Lee et al.[72] and a negative sign appears in the eqn. (1.10).

It can be seen that eqn. (1.10) (without negative sign) gives the values of the sine term as

$$0 \text{ for } n = 0, 2, 4,\ldots..,$$
$$1 \text{ for } n = 1, 5, 9,\ldots..,$$
$$-1 \text{ for } n = 3, 7, 11,\ldots$$

Thus only odd values of n give rise to the maximum and minima in the EXAFS curve, whereas the even values of n correspond to the nodes. Deshpande et al.[73] were therefore led to believe that there has been obviously a mistake in the printing of eqn. (1.10) in the original paper of Lytle et al.[74] (1975). Actually the periodicity of the EXAFS function given by eqn. (1.10) (with negative sign) is governed by

$$-\sin[2kR_i + \delta_i(k)] \qquad (1.18)$$

The maxima and minima for the first coordination shell in EXAFS should therefore be given by

---

[70] Sarode P. R. and Chetal A.R., 1977, J. Phys. C, **9**, 153.
Landge P. R. and Shrivastava B. D., 1979, Nuovo Cimento B, **49**, 118.
Sahastrabudhe V. S., 1985, Indian J. pure and appl. Phys., **23**, 168.
Garg K. B., Jerath K. S., Chauhan H. S. and Chandra U., 1986, Pramana, **27**, 821.

[71] Stohr J., Johansson L., Lindau I., and Pianetta P., 1979, Phys. Rev. B, **20**, 664.

[72] Lee P. A., Citrin P. H., Eisenberger P., and Kincaid B. M., 1981, Rev. Mod. Phys., **53,** 769.

[73] Deshpande A. P., Sapre V. B. and Mande C., 1988, Phys. Stat. Sol. (b), **145**, 77.

[74] Lytle F. W., Sayers D. E. and Stern E. A., 1975(a), Phys. Rev. B, **11,** 4825.

$$(\frac{1}{2} + n)\pi = 2k(R_1 - \alpha_1) + 2\beta_1, \quad (1.19)$$

Where n = 1, 3, 5,… for the maxima and n = 0, 2, 4,…. for the minima.

Although the original L.S.S. theory distinguishes between the K, L_I, L_{II} and L_{III} absorption discontinuities for the analysis of EXAFS data, the graphical approach, however, does not make such a distinction . To generalize this approach for the K and L_I absorption discontinuities which arise from an initial s state, on one hand, and for the L_{II} and L_{III} discontinuities, on the other, which arise from p state, eqn. (1.18) can be rewritten as

$$-\sin[2kR_1 + 2(-\alpha_1 k + \beta_1) - \pi] \quad (1.20)$$

The above expression indicates that eqn. (1.19) should be replaced by

$$(\frac{1}{2} + n)\pi = 2k(R_1 - \alpha_1) + 2\beta_1 - \pi. \quad (1.21)$$

The factor π is absent for the L_{II} and L_{III} absorption discontinuities.

We have extensively used eqn. (1.19) in the present thesis for the analysis of EXAFS data.

1.9.2 Fourier Transform (FT) method

In the present thesis, bond length has also been determined by the Fourier transformation method for the copper salts and copper complexes studied in chapters IV and V. We have, however, determined only the phase uncorrected bond lengths by this method. No attempt has been made to employ the fitting procedures by which phase corrected bond length can be determined, because the required crystallographic data is not available for any of the complexes studied.

One of the earliest analyses of EXAFS was based on the Fourier transform (FT) of the data expressed in momentum space[75]. The absolute value of the transform was found to peak at distances shifted from the known values by 0.2 - 0.5Å. By correcting for these shifts using systems with known distances, bond length information can be extracted.[76]

---

[75] Sayers D.E., Stern E.A., and Lytle F.W., 1971, Phys. Rev. Lett., **27**, 1204.

[76] Stern E.A., 1974, Phys. Rev. B, **10** 3027.
Sayers D.E., Stern E.A., and Lytle F.W., 1971, Phys. Rev. Lett., **27**, 1204.
Lee P.A. and Beni G., 1977, Phys. Rev. B, **15**, 2862.
Kelly S. D., Hesterberg D. and Ravel B., 2008, *Methods of Soil Analysis. Part 5. Mineralogical Methods,* (Soil Science Society of America, Madison, USA), Chapter 14.

The Fourier transformation of $k^n \chi(k)$ in momentum (k) space over the finite k range k_{min} to k_{max} gives rise to a modified radial distribution function $\phi_n(R')$ in distance (R') space.

$$\phi_n(R') = \frac{1}{\sqrt{2\pi}} \int_{k_{min}}^{k_{max}} w(k) k^n \chi(k) e^{2ikR'} dk \qquad (1.22)$$

To locate the position of each peak in $\phi_n(R')$, it is necessary to understand the phase shift more fully. The linear k dependent term shifts the frequency of the sine wave of EXAFS equation from R_i to $(R_i - \alpha_i)$. In the Fourier transform, this has the effect of shifting all the peaks towards the origin by α, where α amounts to 0.2 ~ 0.5 Å depending upon, among others, the elements involved, the E_0 chosen, and the weighting scheme. α can be obtained from model compounds and transferred to the unknown systems to predict distances.

Also included in the Fourier transform is a window function w(k) which select the *k* range to be transformed. w(k) can be square window if care is taken to choose the cutoffs to be where χ(k) is small or a smooth window such as the following Hanning function can be applied.

$$w(k) = \frac{1}{2}\left[1 - \cos 2\pi\left(\frac{k - k_{min}}{k_{max} - k_{min}}\right)\right] \qquad (1.23)$$

It is clear that w(k) = 0 at $k = k_{min}$ and k_{max}. This window is normally applied to the first and the last 5 - 10% of the data while keeping w(k) = 1 for the remaining data set. It is clear that this window smoothly sets the data to zero (w(k) = 0) at k_{min} and at k_{max}.

In general, this method works well for systems with well separated peaks. The weakness of it is that since the amplitude F(k) and the phase Φ(k) functions have characteristic k dependence, the Fourier transform peak magnitude and the phase shift α in the distance space depends on E_0, the weighting of the data, the data range in k space and the Debye-Waller factors etc.

1.9.3 EXAFS analysis using Athena and Artemis softwares

EXAFS spectroscopy provides structural information about a sample by way of the analysis of its X-ray absorption spectrum. It allows determining the chemical

environment of a single element in terms of the number and type of its neighbors, inter-atomic distances and structural disorders. This determination is confined to a distance given by the mean free path of the photoelectron in the condensed matter, which is between 5 and 10 Å radius from the element.

Modeling EXAFS spectra to determine the average, local-molecular coordination environment of an absorber atom is a multi-step process that is learned through hands-on experience. The process of building a structural model is described with specific references to the EXAFS data analysis programs Athena for background removal and Artemis for optimizing the theoretical model to the measured spectrum.

The EXAFS equation contains structural parameters (N, R, σ^2) as well as functions which are characteristic of atoms in the sample (f(k), δ_1(k), λ(k)). These scattering amplitudes an1d phases can be obtained to a good approximation by comparing the unknown sample with standard compounds of known structure; the scattering amplitudes and phases are said to be transferable. The reason that the transferability concept works well is that the backscattering amplitude is relatively insensitive to the potential in the periphery of the backscattered (one way to see this is that the large momentum transfer involved in backscattering can only be caused by high spatial Fourier components of the scattering potential, which occur in the core region of the backscatterer). Since it is the outer regions of the scattered that are affected most by chemical bonding and solid state effects, the scattering amplitudes and phases are not strongly sensitive to chemical effects in the EXAFS region.

The traditional method of data analysis involves a sequence of steps (fig.1.15): correction for instrumental effects such as detector dead time losses and energy resolution; spectrum averaging and removal of monochromator glitches; normalization of the spectrum to unit edge step to compensate for variations in sample thickness or concentration; selection of the energy threshold E_0 and interpolation to k-space; subtraction of smooth background (typically using cubic spline functions) to generate χ(k); Fourier transformation and filtering to produce single shell amplitude and phase; determination of model parameters using the ratio method or nonlinear least squares fitting of data using empirical or theoretical standards. None of the numerical operations is particularly difficult; they are straightforward to implement using standard subroutine libraries.

In Present thesis, the EXAFS data is analyzed to yield structural information using the available computer software Athena.

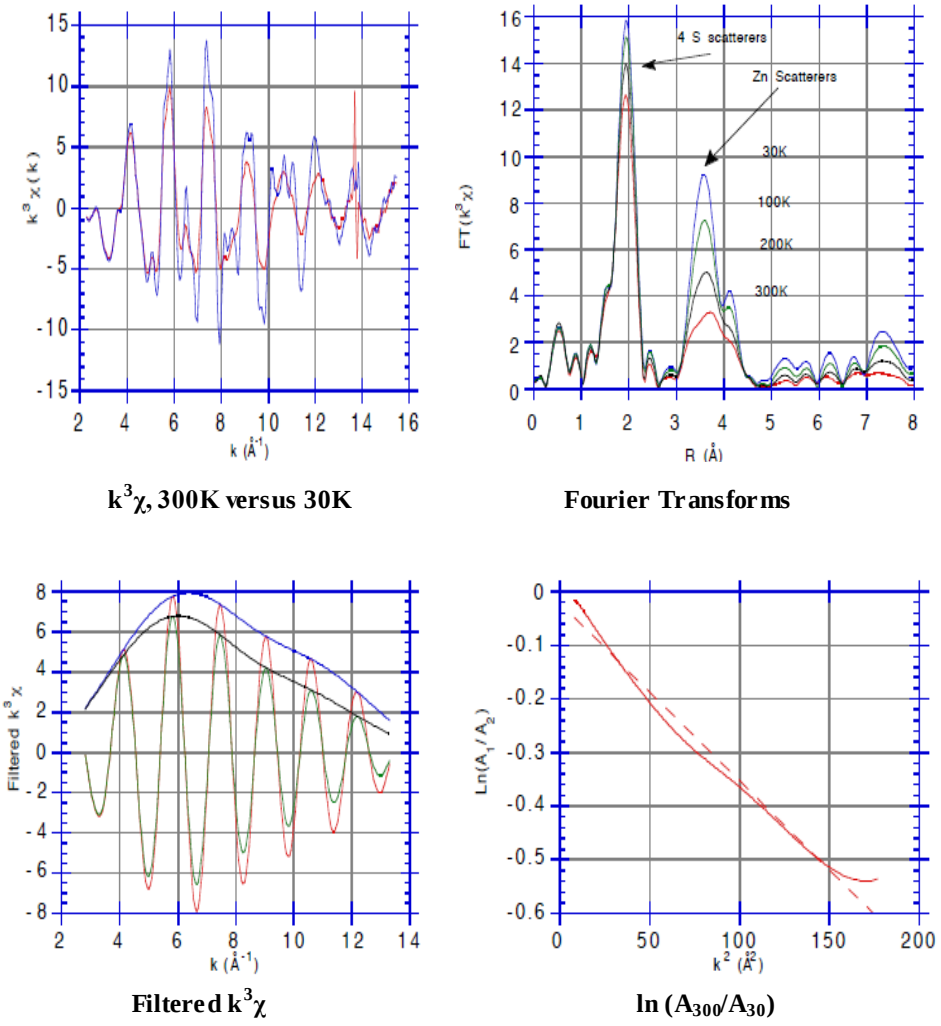

$k^3\chi$, 300K versus 30K **Fourier Transforms**

Filtered $k^3\chi$ **ln (A_{300}/A_{30})**

Figure 1-15 Traditional method of data analysis

1.9.4 EXAFS analysis using MathCAD programming

It has been pointed out above that the commonly used methods of EXAFS data analysis like Artemis require expertise and are time consuming and that the aim of the present work is to describe a simplified EXAFS analysis method using MathCAD programming. The method is given in detail in chapters VI of this thesis. Briefly, the method can be described as follows. In the present method, the theoretical EXAFS spectrum can be calculated using standard EXAFS eqn. (1.10) using MathCAD programming. The phase shift parameter can be also be calculated by L.S.S. (Lytle, Sayers and Stern)[77] method. The other parameters like N, R, σ^2, λ can be taken directly from standard crystallographic tables. χ(k) data can be obtained by varying k

[77] Lytle F. W., Sayers D. E. and Stern E. A., 1975(a), Phys. Rev. B, **11,** 4825.

from 2 to 12 Å in EXAFS equation. The calculated EXAFS data can be compared with experimental curves. These EXAFS data can be Fourier transformed for R range 0 to 6 Å using eqn (1.22). The calculated radial distribution function is plotted versus R and compared with experimental curves. The value of radial distance corresponding to peak position of Fourier transform amplitude gives first shell radial distance from the absorbing atom. But this value is phase shifted. To get actual distance, we have to add α parameter in phase shifted radial distance.

This method has been successfully employed for the transition metals: chromium, manganese, iron, cobalt, nickel, copper and zinc. The experimental EXAFS data for these have been taken from "the EXAFS model compound library" available at (http://cars9.uchicago.edu/~newville/ModelLib/). The data were recorded by using metal foils at room temperature. The method of calculation and the results are given in chapters VI of this thesis. The EXAFS data analysis by this simplified method has also been done on some copper complexes and copper salts the EXAFS data of which were recorded by earlier workers in our own laboratory. The results of such analysis are given in chapter VI of this thesis.

1.9.5 EXAFS spectroscopy using synchrotron radiation

Development of the specialized synchrotron radiation (SR) sources of high brightness affords considerable advancement in using absorption-spectroscopy methods for determining the local atomic and electronic structure of absorbing centers in materials science, physics, chemistry, and biology. The extended X-ray absorption fine structure (EXAFS) spectroscopy is one of the mainstream directions of absorption spectroscopy and allows high-accuracy determination of the parameters of the short-range order in multicomponent amorphous and quasi-crystalline substances.

Rapid advance in the X-ray absorption spectroscopy (XAS) method is caused by appearance of synchrotron sources all over the world, as well as by considerable achievement in the theory and its practical realization in convenient and easily available software packages. XAS can provide information that substantially complements the results of other experimental methods, such as the diffraction (scattering) of X-rays and neutrons, photoelectron, and emission X-ray spectroscopy. The basic XAS advantages are (i) selectivity in the chemical-element type (in some cases, also in the location of an element in a material), which enables one to acquire

information on pair and multi-atomic distribution functions for the local environment of each elements of the material under investigation; (ii) sensitivity to the partial densities of vacant states near the Fermi level; (iii) high density sensitivity (10–100 particles per mole) and relatively short times (from milliseconds to tens of minutes) of detecting experimental spectra when the synchrotron radiation is used; and (iv) a small required sample volume (usually, an amount less than 30 mg/cm^2 is enough). Due to these advantages, the employment of XAS is especially attractive for studying the crystalline and disordered (amorphous, glassy, liquid, and gaseous) multicomponent materials, as well as for carrying out in situ investigations of dynamical processes (phase transitions and chemical reactions).

The use of synchrotron radiation (SR) as a source of a continuous spectrum significantly stimulated the development of EXAFS spectroscopy and its various applications. The SR sources are many orders of magnitude brighter than X-ray tubes and ensure quick (as short as several milliseconds) EXAFS-spectrum measurement for low densities of an element[78]. The first SR sources were designed at the storage rings VEPP-3, Russia, in 1971; ADONE, Italy, 1979; ACO, France, 1970; and SPEAR, Stanford University, California, USA, 1973 (Kunz, 1979, Munro, 1991). At present, the third-generation SR sources ESRF, France; ALS and APS, USA; ELETTRA, Italy; and SPRING8, Japan with radiation brightness up to ~10^{19} photons are in operation. More than 50 sources are now in operation and more than 10 are being designed[79]. Having high brightness and distinct linear or circular polarization, SR provides unique research possibilities. In particular, new XAS methods, which were developed for studying atomic and electronic structures in both the bulk and the surface layers of various thickness values, are as follows:

1. Fluorescent EXAFS (FEXAFS) spectroscopy;
2. Surface EXAFS (SEXAFS) spectroscopy by measuring Auger electrons, the total or partial yield of the photoelectron current, the yield of the photo-induced ion desorption, and the total internal reflection;
3. EXAFS spectroscopy of X-ray excited optical luminescence (XEOL);

[78] Darty, E., Depautex, C., Dubuisson J. M., Fontaine A., Jucha A., Leboucher P., and Tourillon G., 1986, Nucl. Instrum. Methods Phys. Res. A, **246**, 452

[79] Kunz, C., 1979, *Synchrotron Radiation Techniques and Applications*, edited by Kunz C. (Berlin: Springer), p. 1
Munro, I. H., Boardman, C. A., and Fuggle, J. C., 1991, *World Compendium of Synchrotron Radiation Facilities*, (Orsay, ESRS).

4. The method of measuring the circular magnetic X-ray dichroism (CMXD) applicable to the investigation of the magnetic properties of materials (Kincaid, 1975); and
5. EXAFS spectroscopy by measuring the intensities of Bragg peaks-diffraction anomalous fine structure (DAFS).

In the present thesis, X-ray absorption spectra at the K-edge have been recorded for copper complexes and copper salts using the dispersive EXAFS beamline (BL-8) at Indus-2 synchrotron at Raja Ramanna Centre for Advanced Technology (RRCAT), Indore.

1.10 Fourier Transform Infrared Spectroscopy (FTIR)

Fourier Transform Infrared (FTIR) Spectroscopy has been extensively developed over the past decade and provides a number of advantages. Fourier Transform Infrared spectroscopy (FTIR) is widely used in both research and industry as a simple and reliable technique for measurement, quality control and dynamic measurement. FTIR it is most useful for identifying chemicals that are either organic or inorganic. It can be utilized to quantitate some components of an unknown mixture. It can be applied to the analysis of solids, liquids, and gasses. FTIR can be used to identify chemicals from spills, paints, polymers, coatings, drugs, and contaminants. FTIR is perhaps the most powerful tool for identifying types of chemical bonds (functional groups). It is use in forensic analysis in both criminal and civil cases, enabling identification of polymer degradation for example.

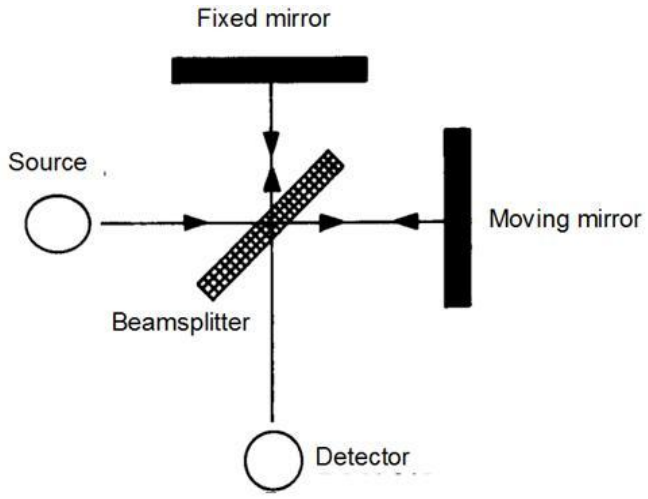

Figure 1-16 Schematic diagram of a Michelson Interferometer.

In infrared spectroscopy, IR radiation is passed through a sample. Some of the infrared radiation is absorbed by the sample and some of it is passed through (transmitted). The resulting spectrum represents the molecular absorption and transmission, creating a molecular fingerprint of the sample. If percentage absorbance or transmittance is plotted against frequencies, then infrared spectrum of the compound is obtained.

Since infrared spectra contain a large number of bands, the possibility that two different compounds will have the same infrared spectrum is exceedingly small. For this reasons an infrared spectrum has been called the "fingerprint" of a molecule. Thus, if two pure samples give different infrared spectra, the compounds must be different. If they give the superimposable spectra then they represent the same compound.

1.11 X-ray powder diffraction (XRD)

X-ray powder diffraction (XRD) is a rapid analytical technique used for phase identification of a crystalline material and can provide information on unit cell dimensions. X-ray powder diffraction is most widely used for the identification of unknown crystalline materials (e.g. minerals, inorganic compounds). Determination of unknown solids is critical to studies in geology, environmental science, material science, engineering and biology. Other applications include characterization of crystalline materials, identification of fine-grained minerals such as clays and mixed layer clays that are difficult to determine optically, determination of unit cell dimensions and measurement of sample purity.

X-ray diffraction is based on constructive interference of monochromatic X-rays and a crystalline sample. These X-rays are generated by a cathode ray tube, filtered to produce monochromatic radiation, collimated to concentrate, and directed toward the sample. The interaction of the incident rays with the sample produces constructive interference (and a diffracted ray) when conditions satisfy Bragg's law[80]:

$$n\lambda = 2d \sin\theta$$

Where d is the spacing between atomic planes in the crystalline phase and λ is the X-ray wave length. These diffracted X-rays are then detected, processed and counted.

[80] Cullity B.D., Elements of X-ray Diffraction, Second Edition,(1978).

The intensity of the diffracted X-rays is measured as a function of the diffraction angle 2ɵ and the specimen's orientation. This diffraction pattern is used to identify the specimen's crystalline phases and to measure its structural properties.

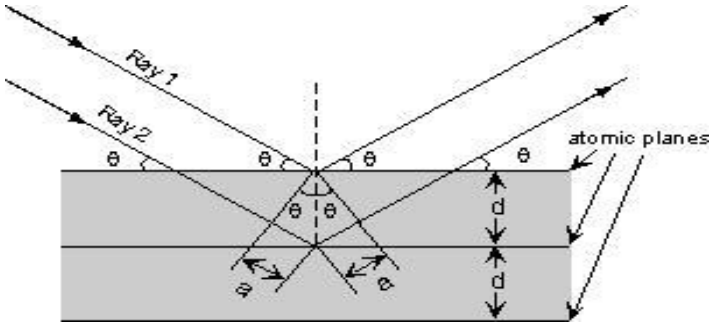

Figure 1-17 Bragg's diffraction

English physicists Sir W.H. Bragg and his son Sir W.L. Bragg developed a relationship in 1913 to explain the basic principal underlying this technique is the Bragg's law of diffraction. It is based on constructive interference of monochromatic X-rays and a crystalline sample. The Braggs were awarded the Nobel Prize in physics in 1915 for their work in determining crystal structure.

1.12 Earlier work done on copper complexes

A survey of the earlier work done on copper complexes reveals that a number of workers have investigated the X-ray absorption spectra at the K-edge of these metals. A number of Ph. D. thesis have been produced on the work done on such complexes. In the following, some of the recent work done on these metal complexes, have been briefly summarized.

Dave M. [81](2000) studied the X-ray absorption spectra on K-edge of copper and cobalt in their hydroxamic mixed ligand complexes. The measurements have been carried out with the help of conventional Seifert's sealed X-ray tube. The XANES parameters, i.e., chemical shift, shift of principal absorption maximum and edge-width etc. have been reported and used to yield information about coordination in the complexes. It was noted that, the K-absorption edge shifts towards the high energy side. From the energy shift of the K-edge (chemical shift), the effective ionic charge on copper atoms in different complexes was reported. The first shell bond length has

[81] Dave M., 2000, *Ph. D. thesis*, Devi Ahilya University, Indore.

also been obtained on the basis of Levy's (1965), Lytle's (1966) and L.S.S. (1975) methods. Dagaonkar N.[82] (2004) has measured chemical shift of X-ray K-absorption edge in some isoxezol mixed ligand complexes of copper possessing +2 oxidation state. It is shown that effective ionic charge is a significant explanatory factor of the variation in chemical shift. Interpretations to the variation in chemical shift are also given on the basis of electronegativity, oxidation state, the valence d-orbital electrons, atomic number, crystal structure etc. The first shell bond length has also been calculated on the basis of Levy's (1965), Lytle's (1966) and L.S.S. (1975) methods.

Awate R. (2009) and Soni N.(2009) studied the K-absorption edge for copper and cobalt pyridine mixed ligand complexes and 3-[N-Phenyle-thiourea-pentanon-2] mixed ligand complexes respectively. They explained the edge position shifts, changes in edge-widths and shifts in the position of first absorption maximum. They also have calculated the bond lengths by using Levy's (1965), Lytle's (1966) and L.S.S. (1975) methods[83] studied X-ray absorption spectra of shiff base copper (II) complexes of 2-(N-aryl ethanimidoyl) mixed ligand complexes. She helps in clarifying the factor affecting the chemical shift in the K-absorption spectra. The XANES (X-ray Absorption Near Edge Structure) technique provides information on distance (in eV) of the principal absorption maxima A with respect to the respective K-absorption edge, edge width, effective nuclear charge and percentage covalancy etc. The EXAFS provides direct, local structural information about the atomic neighborhood of the element[84].

Parsai N.[85] (2011) has studied of absorption spectra of Cu (II) isoxezol and Cu (II) pyridine mixed ligand complexes. In this procedure, the theoretical EXAFS data has been generated, employing computer software MathCAD, for the first coordination shell around the absorbing atom. The K-absorption spectra of some mixed ligand complexes of copper (II) and cobalt (II) with hydroxamic acid as one of the ligands have been investigated. From the Fourier transforms, phase uncorrected bond lengths have been determined (Stern et al.). The bond lengths have also been estimated on the basis of the methods proposed by Levy's, Lytle and L.S.S. (Lytle, Sayers and Stern).

---

[82] Dagaokar N., 2004, *Ph. D. thesis*, Devi Ahilya University, Indore.
[83] Awate Ruchita, Ph. D. Thesis
Soni N., Ph. D. Thesis,2009
Sharma R. Ph. D. Thesis, 2011
[84] Sharma R., Ph. D. Thesis, 2011
[85] Parsai N., Ph. D. Thesis, 2011.

Several research workers have studied copper complexes at School of Studies in Physics, Vikram University, Ujjain from time to time and the results have been presented in their theses. A summary of their studies is given below.

Mool Krishna Gupta (1970), Ashutosh Mishra (1987), Arvind Chandra Gharia (1987), Ramesh Chandra Kumawat (1990), Bhakt Darshan Shrivastava(1996), Rajkumar Katare (2000), Ravindra Kumar Vyas (2006), Ram Dayal Gupta (2006), Vijay Kumar Hinge (2010) and Ajita Johari (2010) and Abhjeet Gour(2012) have studied copper compounds and complexes. They have also summarized in their Ph.D. thesis, the earlier investigations on copper compounds and complexes, available in literature, up to 2013.

International conferences on X-ray absorption fine structure are held in every two-three years. Much of the work on X-ray absorption fine structure is reported in the proceedings of these conferences. Hence, they are a good source for reviewing literature on this subject[86] Proceedings of the XI international conference on X-Ray Absorption Fine Structure XAFS XI, 2000, (Ako, Japan), J. Synchroton Rad., **8**;[87] Hedman and Pianetta, 2007; Andrea Di Cicco and Andriano Fillipponi, 2010).

In our laboratory S Ninama and Garima Jain recently studied the X- ray K-Absorption studies of copper complexes.[88]

1.13 Present work

It is important and interesting to understand the physico-chemical properties of copper complexes with newly synthesized Schiff bases which are of biological interest. The samples of Schiff base ligand have been prepared because they have great biological

---

[86] Stern E. A., 1980, *Laboratory EXAFS Facilities*, (American Institute of Physics, New York).
Teo B. K. and Joy D. C. (eds.), 1981, *EXAFS Spectroscopy Techniques and Applications*, (Plenum Press, New York).
Bianconi A, Incoccia L and Stipcich S (eds.), 1983, *EXAFS and Near Edge Structure* Spring Series in Chemical Physics, **27**, (Springer- Verleg, Berlin).
De Leon J M, Stern E A and Sayers D E, (eds.), 1988, *Proceeding of the V international conference on X-Ray Absorption Fine Structure XAFS V* (Seattle, WA, USA), Physica B, **158**.
Hasnain S S (ed.), 1991, *Proceeding of the VI international conference on X-Ray Absorption Fine Structure XAFS VI*, (Warrington, UK:Daresbury Laboratory).
Kuroda H, Ohta T, Murata T, Udagawa Y and Nomura M (eds.), 1992, *Proceeding of the VII international conference on X-Ray Absorption Fine Structure XAFS VII*, Kobe, Japan, Jpn. J.Appl. Phys., **32**.
Baberschke K and Arvanitis D (eds.), 1994, *Proceeding of the VIII international conference on X-Ray Absorption Fine Structure XAFS VIII* (Freie Universitat, Berlin, Germany), Physica B, **208** & **209**.
Coulon-Ginet C and Brookes N B (eds.), 1996, *Proceeding of the IX international conference on X-Ray Absorption Fine Structure XAFS IX*, (Grenoble, France), J. de Physique IV, **7.**

[87] Hedman B and Pianetta P (eds.), 2007, *Proceeding of the XIII International Conference on X-Ray Absorption Fine Structure XAFS XIII*, (American Institute of Physics, New York) CP **882**.
Andrea Di Cicco and Andriano Fillipponi (eds.), 2010, J. Phys., Conf. Series, **190**.
Andrea Di Cicco and Andriano Fillipponi (eds.), 2010, J. Phys., Conf. Series, **190**.

[88] S Ninma., Ph. D. Thesis, 2013, Garima Jain., Ph. D. Thesis, 2014 DAVV, Indore.

importance, and have found application as antifungal, antibacterial, antitumor, polymers, antifertility and dyes etc.In the present thesis, X-ray absorption fine structure (XAFS) and Extended X-ray absorption fine structure studies (EXAFS) of copper(II) Schiff base complexes **(**Bis-pentanyl R(substituted anilene)- phenyldiazine Cu(II) bis-benzenediamine) and five copper salts have been done. The X-ray absorption fine structure measurements were performed at recently developed BL-8 Dispersive EXAFS beamline at 2.5 GeV INDUS-2 Synchrotron Radiation Source at RRCAT, Indore, India. In XANES Measurements have been made to obtain the chemical shift, edge width, shift of principal absorption maximum and effective nuclear charge (ENC) for these compounds have been used to explain the structure of the complexes. The bond lengths called "nearest neighboring distance" have also been obtained by Levy's, Lytle and L.S.S. (Lytle Sayers and Stern) methods of EXAFS data analysis using with computer software IFEFFIT (*Athena* version 0.8.056). Copper (II) complexes were synthesized by chemical root method. The K-absorption spectra of some mixed ligand complexes of copper (II) have been investigated in the present work. In the present work, the X-ray absorption spectra at the K-edge of the same complexes and same salts were recorded at the recently developed BL-8 dispersive EXAFS beamline at 2·5 GeV Indus-2 synchrotron radiation source at RRCAT, Indore, India. The μ (E) versus E spectra have been normalized, the EXAFS function χ(k) versus k curves have been obtained which have been Fourier transformed. From the Fourier transforms, phase uncorrected bond lengths have been determined (Stern et al., 1975). The bond lengths have also been estimated on the basis of the methods proposed by Levy[89], Lytle[90] and L.S.S.[91] (Lytle, Sayers and Stern). The results of these studies are given in chapters IV and V of this thesis.

The Cu (II) complexes were also characterized by X-ray diffraction (XRD) and Fourier Transform Infrared Spectra techniques. XRD is a resourceful, non-destructive technique that explains the perfect information about the chemical

[89] Levy R. M., 1965, J. Chem. Phys., **43**, 1846.
[90] Lytle F.W., 1966, Advances in X-ray Analysis, **9**,398
[91] Lytle F. W., Sayers D. E. and Stern E. A., 1975(a), Phys. Rev. B, **11,** 4825.

composition and crystallographic structure of natural and manufactured materials. The XRD measurements were carried out using Bruker D8 Advance X-ray diffractometer. Fourier Transform Infrared spectroscopy (FTIR) is one of the most powerful analytical techniques which provide information on molecular vibrations or more precisely on transitions between vibrational and rotational energy levels in molecules. It is used in identify unknown materials present in a specimen. The FTIR measurements were carried out in IUC,DAVV, Indore. In addition, these studies support each other and help to propose the geometry of prepared molecule. The results of these studies are given in chapters III of this thesis.

Also in the present work a simple and innovative procedure for analysis of EXAFS data has been presented[92]. In this procedure, the theoretical EXAFS data has been generated, employing computer software MathCAD, for the first coordination shell around the absorbing atom, using standard EXAFS eqn. (1.10)[93]. The results of such a study are given in chapter VI of this thesis. Theoretical EXAFS data have been generated using standard EXAFS equation employing MathCAD programming. The phase shift parameter has been computed from experimental spectra itself. The results of such a study are given in chapter VI of this thesis.

References to all the chapters have been given at the end of the thesis. In the appendix, copies of the research papers published by the author have been appended.

***

[92] Mishra A., Parsai N. and Dagonkar N., 2009, Indian J. Pure and Appl. Phys., **47,** 337.
Mishra A., Parsai N., Soni N. and Awate R., 2010, Indian J. Pure and Appl. Phys., **48**, 81.

[93] Rehr J. J. and Albers R. C., 2000, Rev. Mod. Phys., **72**,621.
Levy R. M., 1965, J. Chem. Phys., **43**, 1846.